Colloidal transport of carbon and metals by western Siberian rivers during different seasons across a permafrost gradient

Ivan V. Krickov, Oleg S. Pokrovsky, Rinat M. Manasypov, Artem G. Lim, Liudmila S. Shirokova, Jerome Viers

Colloidal transport of carbon and metals by western Siberian rivers during different seasons across a permafrost gradient

Ivan V. Krickov[1], Oleg S. Pokrovsky[2]*, Rinat M. Manasypov[1], Artem G. Lim[1], Liudmila S. Shirokova[2,3], Jerome Viers[2]

[1] *BIO-GEO-CLIM Laboratory, Tomsk State University, Tomsk, Russia*

[2] *Geoscience and Environment Toulouse, UMR 5563 CNRS, Avenue Edouard Belin, 31400, Toulouse, FRANCE*

[3] *Institute of Ecological Problems of the North, Ural Branch of Russian Academy of Science, Arkhangelsk, Russia*

**corresponding author, email: oleg.pokrovsky@get.omp.eu*

Submitted to *Geochimica Cosmochimica Acta*, after revision, August 2019

Abstract

In contrast to fairly good knowledge of dissolved (< 0.45 µm) and particulate (> 0.45 µm) fluxes of carbon, nutrients and metals from the land to the ocean, colloidal (1 kDa - 0.45 µm) forms of solutes are rarely quantified. This is especially true for Siberian rivers draining into the Arctic Ocean: because of organic-rich soils, colloidal fractions of elements are high and may sizably impact coastal biological processes. However, the main environmental parameters such as seasons, river size, climate, permafrost distribution and landscape parameters of the watershed controlling colloidal distribution of organic carbon (OC) and metals remain totally unknown. Here we used on-site centrifugation combined with ultrafiltration via 3, 30 and 100 kDa pore size membranes and 1 kDa dialysis to characterize colloidal size fractionation of OC and metals in 32 western Siberian rivers, ranging in size from 10 to 150,000 km² watershed area, across a climate and permafrost gradient (from absent to continuous permafrost). The dominant forms of OC and metals was low molecular weight $LMW_{< 3\ kDa}$ fraction and medium molecular weight ($MMW_{3kDa\text{-}30\ kDa}$) colloids. The $LMW_{< 3\ kDa}$ fraction of OC increased in the order spring < autumn < summer, following progressive replacement of allochthonous medium and high molecular weight colloids in spring by autochthonous LMW organic ligands in summer; the latter possibly occurred due to exometabolites of plankton and periphyton. The LMW OC fraction became low again in autumn, presumably due to appearance of allochthonous DOM washed out by autumn rains from peat soil at maximum thawing depth. The size of the watershed had subordinate influence on colloidal distribution compared to seasons. The effect of landscape parameters of the watershed on the colloidal status of solutes was subordinate to seasonal and permafrost-zone controls. Overall, the ongoing environmental changes in WSL will likely decrease the proportion of mineral (Fe, Al - bearing) colloids of C and trace metals exported by rivers to the Kara Sea. As a result, the flux of dissolved C, micro-nutrients and metal toxicants may become increasingly bioavailable to coastal aquatic biota.

1. Introduction

Due to the high importance of the Arctic Ocean and permafrost-dominated sub-arctic continental zones in Earth's carbon cycle and the high vulnerability of circumpolar zones to the climate warming, numerous works have been devoted to biogeochemistry of dissolved and particulate organic carbon as well as major and trace elements in large Arctic rivers (Gordeev et al., 1996, 2004; Dittmar and Kattner, 2003; Magritsky, 2010, Holmes et al., 2000, 2001, 2012; Tank et al., 2012; Drake et al., 2018). At the same time, main factors controlling the colloidal status of C and major and trace elements in watersheds of the Arctic Ocean, and their response to climate change are in the preliminary stages of our understanding.

Colloidal transport of organic carbon (OC) and trace metals in continental waters remains a hot topic in earth surface biogeochemistry despite the sizeable amount of effort devoted to characterizing OC, nutrient and metal distribution among particles and colloids (Aiken et al., 2011; Aufdenkampe et al., 2011; Philippe and Schaumann, 2014; Gottselig et al., 2017). Colloids, operationally defined as few nm (1 kDa) - 0.45 μm, and truly dissolved or the low molecular weight ($LMW_{< 1\ nm}$) fraction of total dissolved (< 0.45 μm) riverine load, are a major forms of element migration from land to ocean. In this regard, colloids in high-latitude boreal and subarctic zones have received particular attention given their primary importance in C and micronutrient regulation in the Arctic Ocean as well as their vulnerability in the face of on-going changes (Ingri et al., 2000; Stolpe et al., 2013b; Pokrovsky et al., 2016b; Cuss et al., 2018). However, the environmental factors controlling organic carbon (OC) and trace elements (TE) distribution among different colloidal pools and their change over the hydrological seasons still remain poorly understood. Quantitative prediction on the evolution of colloidal and LMW fraction transport of solutes to the ocean under on-going environmental change (climate warming and human impact) is not yet possible.

74 The reason for this knowledge gap is due to the diversity of dissolved organic matter
75 (DOM) depending on seasons, river size and landscape environments; thus, the difficulty in
76 predicting the nature of organic complexes and the proportion of conceptually different
77 allochthonous (terrestrial) and autochthonous (aquagenic) DOM. This is especially true for small
78 rivers and streams where variable residence time of water and solutes diversify the degree of
79 processing of DOM and DOM-metal complexes and colloids via bio-degradation, photolysis and
80 uptake / release by plankton and periphyton.
81 The variability of colloidal status of C and metals is most strongly pronounced in high-
82 latitude boreal and subarctic regions, where seasonal aspects (glacial period of low DOM, spring
83 flood of high allochthonous DOM and summer baseflow when plankton and periphyton activities
84 impact the river ecosystems) create very complex patterns of C and metal concentration and size
85 fractionation (Bagard et al., 2011, Stolpe et al., 2013a, b; Pokrovsky et al., 2010). Further, in
86 contrast to seawater, where organic complexes and colloidal forms of metals can be assessed by
87 electrochemical techniques (cf., Santana-Casiano et al., 2000), the use of these techniques are
88 very limited in freshwaters (Rozan and Benoit, 1999), and thus the two most common methods
89 of colloidal characterization are size-fractionation using ultrafiltration or dialysis (Vasyukova et
90 al., 2010; Pokrovsky et al., 2016a), and on-line field-flow fractionation coupled to ICP-MS
91 (Stolpe et al., 2013a, b; Cuss et al., 2017; Zhou et al., 2016). Extensive use of these techniques
92 in arctic and subartic inland waters revealed the dominance of organic and organo-mineral (ferric
93 and aluminous) colloids of low and high molecular weight (LMW and HMW), whose
94 proportions vary strongly depending on season and environmental context (Lyvén et al., 2003;
95 Stolpe et al., 2013; Cuss et al., 2017, 2018; Javed et al., 2017). Further, different techniques and
96 even different methodologies within the same technique may produce different results as, for
97 example, the effective cut-off of a filter depend not only on the size of the colloids but also on
98 the composition and concentration of the colloids, the material of the filter, the volume of water

passed through the filter etc. As such, only using a unified protocol throughout wide range of environmental parameters can provide reliable information on colloidal variation in space and time. Up to now, few studies provided colloidal speciation of OC and metals across the seasons in boreal and permafrost-draining rivers (Porcelli et al., 1997; Ingri et al., 2000; Pokrovsky et al., 2010; Stolpe et al., 2013a, b) and over the climate gradient in permafrost-free zones (Pokrovsky and Schott, 2002). The lack of information on colloidal riverine transport of OC and metals over permafrost gradient does not allow identification of landscape factors controlling this transport of solutes in rivers and prediction of possible transformation of these fluxes under on-going environmental change.

To better understand climatic, permafrost and landscape control on colloidal transport of OC and trace metals in Siberian rivers, we sampled 32 rivers of various size ranges across sizeable climate and permafrost gradient and tested the link between the colloidal / LMW fraction of C and 40 macro- and trace elements and major environmental parameters such as latitude, permafrost distribution, bog and forest coverage for 3 main hydrological seasons of the year. As specific hypothesis of this work, first, we suggested that allochthonous (terrestrial) DOM from soil and vegetation leaching would dominate large-size colloids during spring flood whereas autochthonous (aquagenic) DOM and LMW complexes of C and metals may be pronounced during summer baseflow. Second, it was anticipated that the variation in Fe:C ratio in the colloidal fraction would be primarily dependent on river size (different degrees of underground discharge via hyporheic feeding in the PF zone), seasons, and proportion of bogs and forests at the watershed. Third, we anticipate tracing the increase in active layer thickness (ALT) due to permafrost thawing and enhanced mobilization of colloidal OC and metals from deep frozen horizons through comparison of colloidal speciation at the beginning and the end of the active season. Lastly, using a “substitution of space for time” approach, we predict the future changes

123 in colloidal pattern of OC and metals in WSL rivers and their export fluxes based on
124 contemporary features of dissolved riverine colloidal load.
125
126 **2. Study site and methods**
127 *2.1. Rivers of Western Siberian Lowland*
128 We sampled 32 rivers that belong to the Ob, Pur and Taz watersheds in the Western
129 Siberia Lowland. WSL is a huge peatland (> 2 million km²) situated within the taiga forest,
130 forest-tundra and tundra zones. A map of studied rivers is illustrated in **Fig. 1** and their pertinent
131 climatic and physio-geographic characteristics are presented elsewhere (Krickov et al., 2018).
132 The climate gradient of sampled rivers presents a decrease in mean annual air temperature
133 (MAAT) from -0.5°C in the south (Tomsk region) to -9.5°C in the north (Arctic coast). Annual
134 precipitation is fairly constant ranging between 550 mm in the south and 600 mm at the lower
135 reaches of the Taz River. Because of the strong decrease in evapotranspiration northward, the
136 annual river runoff gradually increases from 160-220 mm y^{-1} in the permafrost-free region to
137 280-320 mm y^{-1} in the Pur and Taz river basins located in the discontinuous to continuous
138 permafrost zone (Nikitin and Zemtsov, 1986). Permafrost distribution also follows the MAAT
139 gradient: from absent through isolated and sporadic in the south to discontinuous and continuous
140 in the north. The landscape parameters of sampled catchments were determined by digitizing
141 available soil, vegetation, lithological and geocryological maps (Pokrovsky et al., 2016b;
142 Vorobyev et al., 2017). Sampling was performed during spring flood (17 May – 15 June 2016),
143 summer baseflow (1 – 29 August 2016), and autumn baseflow before ice (24 September – 13
144 October 2016) and covered three main hydrological seasons. Note that the collected data set of
145 colloidal and LMW fraction of WSL river load is unique and independent from previous studies
146 of 'bulk' dissolved (< 0.45 µm) WSL river load assessed during several seasons from 2013 to

147 2015 (Pokrovsky et al., 2015, 2016b) and particulate (> 0.45 µm) and dissolved fraction of these
148 rivers from May through October 2016 (Krickov et al., 2019).
149
150 *2.2. Colloidal separation and analyses*
151 All the analytical approaches used in this study followed methods developed for western
152 Siberian DOM-rich waters (Pokrovsky et al. 2016a, b; Shirokova et al. 2013). In this work we
153 define colloids as entities having the size between 0.45 µm and 3 kDa. Further, we distinguish
154 two group of high-molecular weight (HMW) ($HMW_{100\ kDa\ -\ 0.45\ \mu m}$ and $HMW_{30\ kDa\ -\ 100\ kDa}$),
155 medium molecular weight (MMW) colloids ($MMW_{3kDa\ -\ 30\ kDa}$), and low molecular weight
156 (LMW) fraction ($LMW_{<\ 3\ kDa}$).
157 Approximately 1 L of unfiltered surface water was collected in pre-cleaned light-
158 protected polypropylene jars for size fractionation to 0.45 µm followed by a centrifugal, non-
159 cascade, ultrafiltration through 100, 30 and 3 kDa NMWL single-used Amicon Ultracell 15-mL
160 cartridges. These disposable 50-mL polypropylene vials were fitted with regenerated cellulose
161 filters which were first treated with 1% HNO_3, and rinsed 3 times via passing between 50 and
162 100 mL of MilliQ water through the membrane. The DOC and metal blanks were a factor of 3
163 to 10 lower than the minimal concentrations of these components in experimental fluids. The
164 first portion of sample supernatant that passed through Amicon cartridges was rejected. Each
165 fraction of filtrate was sub-devised into non-acidified and acidified portions, for carbon/pH and
166 trace element measurements, respectively. The centrifugal ultrafiltration was run at 20°C using
167 Eppendorf 5920 centrifuge (4000 rpm, 20 min). Vacuum filtration was performed using a
168 Mityvac MV8255 PVC-made hand pump. The filtration and ultrafiltration allowed for separation
169 into two group of high-molecular weight colloids ($HMW_{100\ kDa\ –\ 0.45\ \mu m}$ and $HMW_{30\ kDa\ -\ 100\ kDa}$),
170 MMW colloids ($MMW_{3kDa-30\ kDa}$), and LMW fraction ($LMW_{<\ 3\ kDa}$). The concentrations of

elements in the different size fractions were calculated from the differences between concentrations in different filtrates.

All filtrations and colloidal separations were run on site, in a protected environment, within 2 h of river water collection. Further methodological details and possible artifacts of centrifugal ultrafiltration are described elsewhere (Oleinikova et al., 2017a). In addition to centrifugal ultrafiltration, approximately 30% of river water samples collected in summer and autumn were processed for dialysis separation of colloids and 'truly' dissolved fraction. In-situ dialysis experiments were performed by using 30-ml pre-cleaned dialysis bags (1 kDa or ~1.4 nm, Spectra Por 7®), which were placed directly in the river water for 3 days following previous methodologies (Pokrovsky et al., 2016a). The major and trace element composition of the lake water remained stable (± 10%) in the course of the dialysis procedure, as verified by 0.45 µm filtration before and after exposure.

The pH was measured in-situ. Chloride and sulfate were measured by ion chromatography (Dionex 2000i) with an uncertainty of 2%. The concentrations of DOC and DIC were determined by using a Shimadzu TOC-VSCN Analyzer with an uncertainty of 3% and a detection limit of 0.1 mg/L. All elements were measured without preconcentration with an ICP-MS Agilent 7500 ce using the collision cell with helium and hydrogen gas (He and H mode) to diminish the interferences. Indium and rhenium were used as internal standards at concentrations of ~3 µg/L and corrections from polyatomic spectral interferences were made for rare earth elements (REEs) and the other trace elements. The typical uncertainty for elemental concentration measurement ranged from 5-10 % at 1-1000 µg/L to 10-20 % at 0.001 – 0.1 µg/L. The MilliQ field blanks were collected and processed to monitor for any potential sample contamination introduced by our sampling and handling procedures. The organic carbon blanks of filtrates and ultrafiltrates never exceeded 0.1 mg/L. For all major and most trace elements, the concentrations in the blanks were below analytical detection limits (≤ 0.1-1 ng/L for Cd, Ba, Y, Zr, Nb, REE, Hf, Pb, Th, U; 1 ng/L

for Ga, Ge, Rb, Sr, Sb; ~ 10 ng/L for Ti, V, Cr, Mn, Fe, Co, Ni, Cu, Zn, As). The international geostandard SLRS-5 (Riverine Water Reference Material for Trace Metals) was used to check the validity and reproducibility of analysis. No dilution of SLRS-5 was necessary to match the concentrations of DOC- and TE-rich Siberian river samples. All certified major (Ca, Mg, K, Na, Si) and trace elements (Al, As, B, Ba, Co, Cr, Cu, Fe, Ga, Li, Mn, Mo, Ni, Pb, all REEs, Sb, Sr, Th, Ti, U, V, Zn) concentrations of the SLRS-5 standard and the measured concentrations agreed with an uncertainty of 10-20%. The agreement with SLRS-5 for Cd, Cs and Hf was between 30 and 50%, although the uncertainty on the analyses of these elements was between 5 and 10%.

Statistical analysis was used to quantify the relationship between major and trace element proportion in colloidal or $LMW_{< 3\ kDa}$ fraction and % of permafrost, amount of wetlands/lake/forest coverage in the watershed, and the surface area of the watershed ($S_{watershed}$). Note that applying correlation analysis to proportions can lead to the detection of apparently significant "spurious correlations", since an increase in the proportion of a given constituent may be caused by the increase in the amount underlying that proportion, a decrease in other proportions, or both (e.g., Pawlowsky-Glahn and Buccianti, 2011). To add certainty, we used a confidence level of 99% ($p < 0.01$). We also tested the correlations between element concentrations in the $LMW_{< 3\ kDa}$ fraction and the physio-geographical parameters of watershed; the dependencies were essentially the same. However, since the absolute concentrations in WSL rivers are strongly affected by season and latitude (i.e., Pokrovsky et al., 2016b), we chose to show the % fractions for better representation of environmental impact on colloids across various seasons and permafrost zones.

Similar to previous work in this region, we distinguished five zones of permafrost distribution in river watersheds: 1) permafrost-free zones located south of 61°N latitude, 2) isolated zones located between 61 and 63.5°N latitude; 3) sporadic zones located between 63.5 and 65°N latitude; 4) discontinuous zones located between 65 and 66°N latitude, and 5)

continuous permafrost zones located north of 66°N latitude. Correlations between element concentration in various colloidal fractions, the relative proportion of these fractions and main parameters of the watershed (latitude, watershed area, runoff, percentage of bogs, forest and lakes and the permafrost coverage) were tested using both Pearson and Spearman coefficients at $p < 0.05$ for rivers of different size ranges (< 100 km², 100-1000 km², 1000-50,000 km², and > 50,000 km²) during each season as well as for all 3 seasons simultaneously.

3. Results

3.1. Impact of river size, season, latitude and permafrost distribution on colloidal (3 kDa - 0.45 µm) fraction of C and TE.

The concentrations of elements in 5 main fractions (< 1 kDa, < 3 kDa, < 30 kDa, < 100 kDa and < 0.45 µm) averaged over permafrost-free and permafrost-bearing rivers for each season are listed in **Table 1** whereas all raw data for each river are provided at the Research Gate repository (Pokrovsky et al., 2019). Considering all available rivers and dissolved components, no distinct link between $S_{watershed}$ and concentration of colloids or proportion of LMW fraction could be established ($R_{Pearson}$ is not significant at $p < 0.05$). However, several elements exhibited distinct impact from river size on colloidal (3 kDa - 0.45 µm) fraction. There was a decrease of colloidal fraction of Al, Fe, Ca, P, Mo and U with increase in watershed size, this was especially visible in summer and autumn (**Fig. 2 A-F**). The organic carbon (OC) and divalent metals (Ni, Cu, Mn, Co, Cd, Pb) did not exhibit any statistically significant impact from watershed size on colloidal fraction (not shown). The pattern of element colloidal fraction with latitude or permafrost zone was distinctly different during the 3 seasons studied. In spring, the 80±20% of colloidal DOC in rivers in the permafrost-absent zone decreased to 20-40% reaching the same proportion as in rivers located north of 66°N, in the continuous PF zone (**Fig. 3 A and Fig. S1 A**). The colloidal DOC increased from S to N during the summer period (**Fig. S1 B**); this pattern

was pronounced in rivers larger than 100 km² also in autumn (**Fig. S1 C**). Al demonstrated systematic decrease of colloidal fraction in PF-free rivers (south of 60°N) in the order spring > summer > autumn; this decrease was also detectable in rivers from permafrost zone (**Fig. 3 B**), north of 60°N (**Fig. S2 A-C**). Fe was essentially present (> 90%) in colloidal forms in permafrost rivers (**Fig. 3 C**). In contrast, in rivers from permafrost-absent zones, the Fe colloidal fraction decreased over active seasons from 95-98% in spring to 10-40% in autumn (**Fig. 3 C, S3 A-C**). Ca, Mg and P also demonstrated the highest fraction of colloids in spring and the lowest fraction of colloids in summer and autumn, especially visible in permafrost-free zones (**Fig. 3 D, E and F**, respectively).

There was a decrease in colloidal forms of low-soluble trivalent and tetravalent (Ti, Zr, Hf, Th, Ga, Y, REE) elements in summer compared to other seasons, which was visible across all permafrost zones (**Fig. S4**). The divalent metals (Cu, Ni, Co, Mn, Cd, Pb) exhibited a much higher colloidal fraction in spring compared to summer and autumn, detectable throughout all permafrost zones (**Fig. S5**). Neutral molecules, oxyanions and U(VI) demonstrated a similar pattern, although colloidal forms of U were especially low in summer and autumn in the permafrost-free zone **(Fig. S6**).

Note that suspended matter concentration in WSL rivers strongly increases during spring flood (Krickov et al., 2019). This can potentially produce so called "particle concentration effect" (Benoit and Rozan, 1999) thus influencing the distribution of colloids amongst the different size fractions, biasing it towards higher proportions in smaller size fractions. However, the proportion of small size fraction of many elements (Al, Ca, Mg, P, divalent metals) was the lowest in spring, which is contrary to what is expected if particle concentration effect could bias the distribution of colloids.

3.2. Dependence of colloidal fraction on forest and bog coverage in the watershed

Spring period was characterized by minimal links of element colloidal fraction and watershed parameters such as forest and bog coverage (**Fig. 4**). In the summer and autumn, the colloidal fraction for a number of highly mobile elements (all alkalis (Li, Na, K, Rb) and alkaline-earths (Mg, Ca, Sr, Ba), Co, Ni, As, and Mo) decreased with the degree of forest coverage in the drainage basins. In autumn, the effect was also visible for Al, P, Ti, Th. Other elements did not demonstrate any significant ($p < 0.05$) link of their colloidal fraction to forest coverage of the watershed. Bogs exerted a rather weak control on colloidal forms of elements: DOC weakly increased in spring but had no effect in summer and autumn (**Fig. 5 A**). Alkalis and alkaline-earth elements increased their colloidal fraction with bog increase in summer and autumn **(Fig. 5 B-D**). For all other elements, the effect of bog coverage was not detectable within the variations between different rivers (not shown). Note that, given relatively low coverage of WSL territory by lakes (~6%, Polishchuk et al., 2017), the role of lake in river watershed on element status in colloids was strongly subordinate relative to bogs and forests, and as such not considered in interpretation of results.

3.3. Fe:C stoichiometry of colloids

The stoichiometry of Fe:C ratios in colloidal (3 kDa - 0.45 µm) and $LMW_{< 3\ kDa}$ fractions depended primarily on latitude and season, but were much weaker affected by landscape parameters. Thus, watershed size had little effect on Fe:C ratio in colloidal fraction ($R^2 < 0.2$-0.3, **Fig. 6 A**) and the Fe:C ratio in $LMW_{< 3\ kDa}$ fraction followed the order autumn > summer > spring (**Fig. 7 A**). The Fe:C ratio in colloids $(Fe:C)_{3\ kDa\ -\ 0.45\ \mu m}$ increased with latitude in spring ($R^2 = 0.50$, $p < 0.01$, **Fig. 6 B**) whereas this ratio in the LMW fraction $(Fe:C)_{<3\ kDa}$ decreased northward in spring and summer (**Fig. 7 B)**. Forest coverage yielded weak enrichment in Fe relative to C in colloids in summer and autumn (**Fig. 6 C**) but the effect was absent in spring (not

shown). No clear effect of forest coverage on Fe:C ratio in the $LMW_{< 3\ kDa}$ fraction was revealed although there was some increase of this ratio (R^2 = 0.40±0.03) in rivers of 100-1000 km² watersheds in autumn (not shown). Finally, the bogs and lakes in the watersheds exhibited no effect on Fe:C ratio in colloids and LMW fraction of river water (not shown).

3.4. Size fractionation of colloids

Dialysis through 1 kDa membrane and Amicon centrifuginal ultrafiltration (3 kDa) performed in summer and autumn demonstrated virtually identical (within ± ≤10%) concentrations of C and metals in 1 kDa and 3 kDa size fractions. This strongly suggests that the LMW colloidal fraction having the size between 1 kDa and 3 kDa represents less than 10% of DOC and < 2-5% of all other elements (**Fig. S7 A-H**). This fraction therefore has negligible impact on colloidal speciation and $LMW_{< 3\ kDa}$ obtained by centrifugal ultrafiltration for all WSL rivers in this study is thus equivalent to the more frequently used $LMW_{< 1\ kDa}$ cutoff. The distribution of elements between different colloidal fractions demonstrated a dominance of $LMW_{< 3\ kDa}$ 'truly dissolved" forms and medium molecular weight ($MMW_{3\ kDa\ -\ 30\ kDa}$) colloids for most components, regardless of season and permafrost type. These distributions are illustrated in **Fig. 8** for major components of colloids (OC, Al, Fe) and Ca. Organic carbon did not demonstrate any systematic change of colloidal forms over different permafrost zones in summer and autumn, but there was a systematic increase in the $LMW_{< 3\ kDa}$ form and decrease in $MMW_{3\ kDa\ -\ 30\ kDa}$ colloids from PF-free to continuous permafrost zone (**Fig. 8 A-C**). Aluminium demonstrated dominant $MMW_{3\ kDa\ -\ 30\ kDa}$ colloids in spring and appearance of $LMW_{< 3\ kDa}$ colloids in summer and autumn (**Fig. 8 D-F**). There was no change in Al distribution among fractions across various permafrost zones suggesting a primarily seasonal rather than physio-geographical control on Al colloidal status. In contrast, Fe exhibited a sizeable proportion of $HMW_{100\ kDa\ -\ 0.45\ \mu m}$ and $HMW_{30\ kDa\ -\ 100\ kDa}$ colloids in summer and autumn (**Fig. 8 G-I**). However,

in spring, Fe was strongly dominated by $MMW_{3\ kDa\ -\ 30\ kDa}$ colloids similar to other insoluble TE^{3+} elements. An example of element poorly affected by colloids is Ca which was largely dominated by $LMW_{<\ 3\ kDa}$ with a sizeable (30-40%) contribution of $MMW_{3\ kDa\ -\ 30\ kDa}$ colloids in spring and a negligible (< 2%) contribution of high molecular weight $HWM_{30kDa-0.45\ \mu m}$ colloids (**Fig. 8 J-L**). All other elements which were affected by colloids followed these 2 main distribution types, specifically the OC-like or trivalent metal (Fe, Al)-like. Note that the role of Mn in colloidal composition was highly subordinate to that of Fe and Al as the molar ratio Fe : Al : Mn in the 3 kDa - 0.45 µm fraction was typically (1-10) : 1 : 0.01. As such, the change of stoichiometry and TE affinity to main components of colloids can be further assessed by analyzing the progressive decrease of element concentration with respect to that of DOC, Fe and Al during decreasing pore size of fractional separation.

The behavior of main colloidal constituents - OC, Fe and Al - during size separation procedure (0.45 µm → 100 kDa → 30 kDa → 3 kDa (→ 1 kDa)) was distinctly different among the three seasons and various permafrost zones (**Fig. 9**). During spring flood, there was high similarity of Al-DOC and Al-Fe concentration patterns during ultrafiltration; the molar ratio of Fe:Al in colloids was close to 1 regardless of pore size and permafrost zone. During summer baseflow, the colloids became Fe-rich and Al-poor, a pattern which was especially pronounced in continuous PF zone. In autumn, strong differentiation between different permafrost zones was observed as colloids became enriched in Al vs OC and Fe.

As for the trace elements, progressive decrease of TE concentrations in the course of fractionation from large to small pore size exhibited two distinct patterns, depending on elemental affinity to either OC or Fe and Al. Two main features of element behavior during ultrafiltration procedure were noted: (1) the changes of element - OC or element - Fe/Al concentration pattern were similar between all studied permafrost zones including the permafrost-free zone, and (2) this pattern varied depending on the seasons as illustrated in **Fig.**

346 **10** for several typical elements. During spring flood period, alkalis and alkaline-earth elements,
347 V, Mo and U decreased their concentrations in parallel with OC. Siderophilic (Cr, Mn, Co, Ni)
348 and chalcophilic (Cu, Cd, Zn, Pb) elements followed the decrease of Fe/Al rather than OC.
349 Trivalent hydrolysates were tightly associated with Fe and Al (indistinguishable between two)
350 whereas tetravalent hydrolysates were essentially bound to Al over Fe (illustrated for Mg and Hf
351 in **Fig. 10 A**). The changes during summer baseflow consisted of the following: *i*) alkalis and
352 alkaline-earth elements were not controlled by colloids as their concentration remains stable
353 during fractional separation, and *ii*) chalcophilic elements (Cu, Cd, Zn, Pb) followed the pattern
354 of OC rather than Fe/Al (shown as example for Mg and Cu in **Fig. 10 B**). In Fall, new features
355 appeared during the size separation procedure: the role of Fe as a colloidal carrier sizably
356 decreased and the divalent metals (Cu, Cd, Zn, Pb), TE^{3+}, TE^{4+} became associated to Al and OC
357 rather than Fe (shown as example of Co and Hf in **Fig. 10 C**).
358

359 **4. Discussion**

360 *4.1. Season and latitude exert stronger control on colloidal fraction than river size*

361 The working hypothesis of this study was that the percentage of colloidal versus LMW
362 fraction and stoichiometry of Fe:C ratio will be primarily dependent on river size, season and
363 landscape parameters of the watershed. Indeed, the river size is expected to control the degree
364 of underground feeding via discharge of underground anoxic Fe(II)-rich waters in the hyporheic
365 zone (Shim et al., 2017). Generally, the permafrost prevents the hydrological connectivity
366 between the groundwaters and the rivers (Walvoord et al., 2012). It is expected that the river size
367 effect will be mostly pronounced in the permafrost zone due to restricted connection between the
368 rivers and shallow surface waters and the lack of talik (unfrozen underground water path under
369 the river bed) in small rivers (Pokrovsky et al., 2015). Further, the residence time of colloids and
370 LMW fraction in the river strongly depends on $S_{watershed}$ and the biological (heterotrophic

371 degradation of DOM) and physico-chemical (photolysis) processes which are known to be able
372 to strongly modify the colloidal composition of surface waters in boreal and subarctic zones
373 (Oleinikova et al., 2017a, b). The decrease of Fe in the colloidal fraction is indeed observed in
374 summer in watersheds larger than 100 km² (**Fig. 2 B**) which may be due to discharge of LMW
375 Fe(II) ionic forms from underground waters. This discharge is mostly visible at low water level
376 and at the highest depths of unfrozen soil layers. However, in the river water, Fe(II) is likely to
377 be oxidized and coagulate as Fe(III) oxy(hydr)oxide HMW colloids or particles. This is
378 illustrated by the data in **Fig. 8I**, showing that the importance of Fe in large colloids (3-30 kDa
379 and 30 kDa - 0.45 um) increase during summer and autumn in the permafrost zones. Further,
380 analyses of particulate load of WSL rivers demonstrated that Fe concentration in river suspended
381 particles follows the order spring < summer < autumn, which is especially visible in permafrost-
382 absent zone where the underground input is mostly pronounced (Krickov et al., 2019).
383 The decrease in colloidal fraction of soluble, highly mobile elements (Ca, Mg, P, Mo, U)
384 also observed in summer and autumn (Fig. 2) is due to increased connectivity of underground
385 reservoirs enriched in ionic forms of these elements, mostly pronounced in southern rivers, as
386 was suggested from early analysis of < 0.45 µm river load across the WSL (Frey et al., 2007a),
387 which is especially visible during baseflow period (Pokrovsky et al., 2015, 2016b). The other
388 elements (Ga, Y, REE, Zr, Hf, Th, Mn, Cu, Ni, Co, Cd, Pb, As, Sb) as well as OC did not
389 demonstrate sizeable impact of river size on colloidal fraction. Presumably, the mechanisms of
390 organic colloid generation and scavenging are similar across all studied river sizes. This implies
391 that the colloids formed at the watershed or within the soil/groundwater discharge within the
392 river channel are not subjected to further to bio- and photodegradation during their transport in
393 the river channel.
394 The season is likely to control two main sources of colloidal DOM in rivers: 1)
395 allochthonous, large-size molecules from surface vegetation and plant litter leaching and

degradation, which are mostly pronounced in spring during high flow and 2) autochthonous, small size molecules originating from exometabolites of phytoplankton and periphyton in rivers, which are most visible during summer (August). This was reflected by generally higher specific UV-absorbance at 254 nm in spring compared to summer and autumn, as evidenced across all river sizes and permafrost zones (Pokrovsky et al., 2015). Additionally, the late autumn seasons corresponding to maximal active layer thickness may provide the DOM colloids from deep peat horizons typically not visible in spring and summer.

The decrease in colloidal fraction of Fe and Al (**Fig. 3B, C**) and many divalent transition metals such as Cu, Ni, Co, Mn, Cd (**Fig. S5**) from spring to autumn could reflect decrease in concentration of allochthonous large-size colloids at the expense of autochthonous LMW ligands that bond metal cations as is known in other boreal taiga rivers (Pokrovsky et al., 2010; Bagard et al., 2011). Note that this was especially pronounced in the permafrost-free zone, where sufficient production of plant leachate could stabilize LMW Fe, Al and divalent metals. Further, high concentration of aquagenic organic LMW ligands from plankton and periphyton in the southern rivers can stabilize Fe in the LMW fraction. This is consistent with the size distribution of DOC in the autumn shown in **Fig. 8 C**: the DOC is dominated by the LMW fraction in the permafrost-free zone, but it is dominated by colloids in all other zones. Alternatively, southern rivers could have sizeable underground feeding by Fe(II)-rich ground waters interacted with soluble sedimentary rocks (limestones). This enhanced underground input in PF-free rivers can stabilize Fe as carbonate and bicarbonate complexes in the LMW fraction. In the course of the season, progressive appearance of these groundwaters could decrease relative proportion of colloidal metals at the expense of LMW ionic forms. This is seen for Ca, Mg, P (**Fig. 3 D, E, F**), and especially U (**Fig. S6**). For the latter, there was almost a 10-fold decrease in colloidal fraction in summer and autumn relative to spring; this decrease certainly reflected high bicarbonate inputs during baseflow of the WSL southern rivers (Frey et al., 2007a; Pokrovsky et al., 2015). The

presence of bicarbonate changes speciation of U^{VI} from organic and organo-ferric colloids to uranyl carbonate complexes as it was evidenced by seasonal observations across the boreal regions (Pokrovsky et al., 2010; Bagard et al., 2011).

In the permafrost zone, the dominance of colloidal forms (> 90%) of Fe during all seasons essentially reflected river feeding by shallow subsurface waters and supra-permafrost flow over peat soils (**Fig. S 3**) as the underground-sourced Fe(II) is minimal and likely to be quickly oxidized into Fe hydroxide particles and HLW organo-ferric colloids. In contrast, Al demonstrated a notable decrease in colloidal forms from spring to autumn even in permafrost-bearing rivers (compare Figs. **3B** and **3C**). It is possible that, unlike Fe, some mobilization of LMW organic Al complexes from peat soils and shallow mineral layers in permafrost rivers occurred in summer and autumn. The increased importance of LMW-Al during summer and autumn could be a result of that the input of colloidal Al from the top soil decreased, while groundwater-Al remained constant. This is further confirmed by sizeable decrease in Al concentration from spring to summer, visible for permafrost-free rivers; this decrease is much less manifested in the LMW fraction compared to the 0.45 µm fraction and HMW colloids (see **Table 1**). Because the seasonal decrease in colloidal Al was especially pronounced in large rivers ($S_{watershed}$ > 50,000 km², **Fig. 2 A**) we believe the main driving mechanisms of seasonal Al colloidal transformation in large rivers is underground water discharge accompanied by an increase in pH. This can be especially pronounced in southern, permafrost-free rivers of the regions, where carbonate-bearing rocks can provide elevated CO_3^{2-} concentrationы and pH (Pokrovsky et al., 2015) thus transforming insoluble or organically-bound $Al(OH)_3°$ complexes into more mobile truly dissolved $Al(OH)_4^-(aq)$.

Latitude was the major governing factor of colloidal forms of OC, major and trace elements in WSL rivers. This is due to the fact that latitude integrates many other physio-geographical parameters such as permafrost, temperature, precipitation, and forest line. For

example, the increase of colloidal fraction with latitude (northward) could be due to northward decrease of the LMW form input through underground feeding. This occurs due to a general decrease of river connectivity with underground reservoirs northward (Ala-aho et al., 2018); these reservoirs are rich in alkalis, alkaline-earth elements, P and As. The change of underground regime feeding, already evidenced for bulk dissolved (< 0.45 µm) major and trace elements (Pokrovsky et al., 2015, 2016), is the most likely explanation for this observed tendency.

A decrease in colloidal DOC in rivers north of 66°N observed in spring (**Fig. 3A, S1 A**) could be linked to colloid coagulation and production of LMW organic ligands during freezing-thawing cycles, as is established for permafrost mire waters located in landscape contexts similar to that of WSL (Pokrovsky et al., 2018). Because WSL rivers in the north freeze solid in winter (Pokrovsky et al., 2015), the decrease in colloidal fraction could be linked to this cryo-transformation of colloids. In summer, the southern rivers have shown a generally lower colloidal fraction compared to northern rivers (**Fig. 3A, S1 B**). We interpret this difference as resultant of two main processes: *i*) thawing of peat and release of colloidal OC in the north, which does not occur in the south and *ii*) leaching of LMW OC and metal complexes from abundant plant biomass and LMW exometabolite production by macrophytes, plankton and periphyton in the south. The increase in colloidal fraction of OC in rivers of the permafrost-free taiga zone (south of 60°N) in autumn compared to summer could be interpreted as due to cessation of in-stream primary production and enhanced leaching of HMW OC from peat bogs and from the bottom horizons of peat soil. Indeed, an increased importance of LMW-DOC relative to colloidal-DOC going from the permafrost-absent to isolated, sporadic, discontinuous and continuous zones. could be due to differences in the composition of terrestrial DOM. The latter reflects the differences in vegetation (tundra versus forest) along the S - N gradient. Forests will produce DOM with more lignin, thus larger in molecular size and this is expected to be mostly pronounced in autumn, during litter fall. Note that, while there was a strong contrast between

colloidal speciation of many elements between permafrost-free and permafrost zones, permafrost type distribution *per se* (isolated, sporadic, discontinuous and continuous) weakly impacted the proportion of colloids.

4.2. Weak role of watershed landscape parameters on colloidal status of elements

The lack of watershed parameters impact on colloidal metals in spring (**Figs. 4, 5**) is presumably due to strong integration of catchment surface conditions during this high flow period. The dominance of surface flow occurring over frozen upper peat horizons and similarity of wetlands ground vegetation (moss, lichens, dwarf shrubs, etc.) across WSL create quite homogeneous conditions that define elemental distribution among colloids and $LMW_{< 3\ kDa}$ forms.

The negative effect of forest coverage on colloidal transport of alkalis and alkaline-earth elements and also As, V and P in summer and autumn (**Fig. 4**) is interpreted as due to increase in depth of the water path under forests which thereby increases connectivity between groundwater and the river (Ala-aho et al., 2018a). The impact of forest coverage is especially pronounced in the permafrost zone because it creates optimal conditions for soil thaw and enhances input of groundwater constituents to the river (Krickov et al., 2018). Deepening of the active layer increases the connectivity of rivers with underground reservoirs and thus enhances mobilization of soluble, highly mobile elements (Li, K, Rb, Ca, Mg, Sr, Ba, As, V, P, Mo) in ionic form to the river. As a result, the colloidal fraction of these elements decreased with increased forest coverage. Note that this underground feeding effect was mostly pronounced in autumn when surface flow through organic soil and peat horizons was minimal and river discharge was low.

The effect of forest coverage on Al, Ti, Y and other trivalent and tetravalent hydrolysates is different from that exerted on the soluble elements. Trivalent and tetravalent hydrolysates

could be mobilized from bottom mineral horizons that become progressively available in the course of summer and autumn as the active layer deepens over the organic horizon to underlying mineral deposits. The effect of forest coverage on TE^{3+} and TE^{4+} colloids becomes visible in autumn (**Fig. 4 G, H**), with maximal active layer thickness and minimal feeding of rivers by lateral peat surface overflow. Loiko et al. (2017) observed similar impact of permafrost thaw when the depth of the active layer moved over the organic into mineral soil horizons in sites of abrupt permafrost thaw in the discontinuous permafrost zones.

The effect of bogs was clearly pronounced only for alkalis and alkaline-earths, which increased their colloidal fraction with bog coverage. There are two possible mechanisms for bogs control on riverine colloids. First, if bogs decrease the connectivity of rivers to underground reservoirs, this will decrease the delivery of alkali and alkaline-earth elements to the river in the form of ionic forms ($LMW_{< 3\ kDa}$) thus increasing relative share of colloidal forms. Note that bogs mobilize colloids during all seasons; however, in summer the autochthonous production of LMW organic colloids in rivers can partially mask the effect of bogs. Second, the generation of colloids in bogs is possible due to photo- and bio-degradation of DOM and DOM-Me complexes from active peat layers. Because of the shallow hydrological connectivity of bogs to rivers (Ala-aho et al., 2018a, b), Fe does not follow OC in these aquatic systems and as a result other elements linked to organo-ferric colloids (P, TE^{3+}, TE^{4+}) did not exhibit any relationship to the bog proportion at the watershed. Only the elements that are complexed to DOM colloids, rather than organo-Fe colloids (i.e., alkalis, alkaline-earths), were impacted by bogs.

4.3. Colloid stoichiometry and element distribution among different colloidal fractions

The ratio of Fe:C in the colloidal (3 kDa - 0.45 µm) fraction is a useful indicator for climate and environmental control on colloid generation in river water. In summer and autumn, there was an appearance of $LMW_{< 3\ kDa}$ fraction of Fe which decreased the relative concentration

of Fe in colloids during this period. The increase in $LMW_{<3\ kDa}$ forms stemmed from *i*) autochthonous production of Fe-organic complexes as evidenced by large rivers of the region (see section 4.1) and *ii*) Fe(II) influx from underground waters in the riparian/hyporheic zones. The latter is confirmed by the fact that the Fe:C ratio in the $LMW_{<3\ kDa}$ fraction was also highest in autumn. The forest coverage increased the amount of Fe in colloids relative to C during this period, likely due to facilitating a connection to the underground source and enhancing Fe-rich colloid formation at groundwater discharge zones within the river bed or the riparian zone. The presence of forest coverage also increased the Fe:C ratio in the $LMW_{<3\ kDa}$ fraction, although this increase was visible solely in rivers having $S_{watershed}$ from 100 to 1000 km².

The distribution of Fe between different size fractions of colloids changed dramatically from spring to summer-autumn in the permafrost zones as shown in **Fig. 8 G, H, I.** This indicates that the source of colloidal Fe changes from spring to summer-autumn. In high-latitude rivers, the primary source of colloidal Fe during spring flood is typically from through leaching of the top soil, while most colloidal Fe during summer and autumn is derived from groundwater input of Fe(II), rapidly oxidizing and precipitating as colloidal Fe(III)-oxyhydroxide. Indeed, the latitude increased Fe:C in colloids during autumn when deep unfrozen water paths became available and more Fe could be discharged to the river from underground and/or shallow subsurface reservoirs. At the same time, the Fe:C ratio in $LMW_{<3\ kDa}$ fraction decreased northward during this period probably due to enhanced production of LMW organic ligands in the north linked to a massive thawing of frozen peat. Such processes have been documented in previous laboratory experiments (Drake et al., 2015; Mann et al., 2015).

An interesting feature revealed by element concentration decrease in the course of ultrafiltration (**Figs. 9, 10**) is the change in the relative role of Fe and Al as colloidal constituents and TE carriers. In spring, the colloids contain similar molar amount of Fe and Al; both of these metals exerted control on a number of TE during size fractionation. In summer, the role of the

546 Al constituent strongly decreased and some divalent metals (Cu, Cd, Zn, Pb) became bound to
547 OC rather than Fe and Al. This may be linked to the appearance of autochthonous organic
548 complexes for these elements. In autumn, the role of Al again became strongly pronounced; this
549 may be due to the increase of the thawing depth and involvement of deep silicate mineral
550 horizons in element mobilization.

551 The $HMW_{30\ kDa\ -\ 0.45\ \mu m}$ colloids of Fe and insoluble TE^{3+} and TE^{4+} elements were
552 dominant during summer and autumn but were in quite low proportion (ca < 20%) during spring
553 (**Figs. 8**). This important observation strongly supports numerous previous findings across
554 permafrost and boreal zones (Pokrovsky and Schott, 2002; Vasyukova et al., 2010; Pokrovsky et
555 al., 2016, Stolpe et al 2013a, b). These studies, performed essentially during baseflow period,
556 suggested HMW Fe-rich colloid generation within the riparian and hyporheic zone due to
557 discharge of partially anoxic deep and shallow ground waters, which contain sizable amount of
558 Fe(II) subjected to oxidation by DOM-rich surface waters. This lead to formation of large
559 molecular size Fe oxy(hydr)oxides, stabilized by organic matter and containing sizeable amount
560 of other trace elements that were co-precipitated with $Fe(OH)_3$ (Pokrovsky and Schott, 2002). In
561 fact, the coagulation of Fe hydroxide with DOM occurs at redox interfaces in peatlands (Riedel
562 et al., 2013) and at the surface of fens (Koretsky et al., 2006). Given the abundance of peatlands
563 in WSL, we believe that these freshly precipitated Fe hydroxides-DOM compounds can become
564 the main source of HMW colloids during baseflow period. The lack of HMW Fe-rich colloids in
565 WSL rivers during spring flood observed in this study is fully consistent with a lack of
566 hydrological connectivity between deep soil and subsurface waters and rivers during this period
567 of the year (Ala-aho et al., 2018a, b). As a result, because the river water cannot pick up Fe(II)
568 from partially anoxic underground and shallow subsurface waters, formation of HMW Fe(III)
569 hydroxide colloids is strongly suppressed and the majority of colloidal flux is dominated by
570 surface runoff generated from leaching of plant litter and upper soil (peat) horizons.

571 *4.4. Foreseeing the evolution of colloidal status of elements in the context of climate change.*

572 The boreal and circumpolar regions of both European Russia and Siberia contain sizeable
573 amounts of OC in peat soil of bog zones and as forest litter of the highly productive taiga zone.
574 As a result, colloids are the main vectors of transport for most trace insoluble and even major
575 elements (such as Ca) the in the boreal zone. Compared to tropical and temperate zones, colloids
576 in boreal zone are 1) richer in Fe(III) and 2) contain a higher proportion of low molecular weight
577 ($LMW_{<1\ kDa}$) labile organic matter (Pokrovsky et al., 2016). It is currently impossible to predict
578 the degree of colloidal export change against changes in soil temperature, permafrost thaw and
579 vegetation zone shifts. However, a direct empirical approach can be efficiently tested for WSL
580 thanks to its unique physio-geographical situation where permafrost and MAAT zones change
581 similarly from south to north.

582 In order to predict the possible evolution of C and metal distribution between colloidal
583 and LMW (potentially bioavailable) pools, a 'substituting space for time' scenario can be applied
584 which is well established in WSL for predicting the evolution of dissolved (< 0.45 μm) C,
585 nutrients and metals concentration and fluxes in rivers (Frey et al., 2007a, b; Pokrovsky et al.,
586 2015; Vorobyev et al., 2017) and soil waters (Raudina et al., 2017, 2018). If permafrost
587 disappears in the sporadic and isolated permafrost zones, this will produce a decrease in riverine
588 colloidal transport of OC, Ca, Mg, P, Fe, Al, Ti, Ni, REEs, As, Mo and U, especially in summer
589 and autumn. The transformation of continuous permafrost into discontinuous and sporadic will
590 not sizably affect colloidal speciation of C and metals, although it is impossible to predict
591 whether or not the contrast between seasons will remain the same or decrease.

592 The role of landscape change (forestation of bogs, drainage of lakes and forest line
593 advancement northward) seems to be lower than that of a permafrost boundary shift northward.
594 However, we expect that the forestation of bogs will inevitably lead to a decrease in colloidal
595 forms of alkalis, alkaline-earth elements, V, P, As, Pb by a factor of 2 to 3. This effect will be

596 mostly seen at the end of active seasons in autumn. Only during this season will the northern
597 rivers become richer in colloidal Fe compared to colloidal C. However, given the relatively low
598 share of autumn flux to the annual C and element discharge by WSL rivers (Pokrovsky et al.,
599 2016), the overall effect of landscape change on colloidal export of solutes from the mainland to
600 the Arctic Ocean may be due essentially to the change in discharge rather than the change in river
601 water colloidal composition and stoichiometry. In the permafrost zone, the increase of the depth
602 of water paths through the organic (peat) horizons into the mineral horizon will bring about an
603 enhanced mobilization of low mobility elements (Fe, Al, other TE^{3+}, TE^{4+}) into the fluid phase.
604 This may enrich riverine colloids in these refractory elements, a process which has been locally
605 observed for sites involving catastrophic thawing of frozen peat (e.g., Loiko et al., 2017).
606

607 **Concluding remarks**

608 Organic and organo-mineral colloids of C and metals in WSL rivers are dominated by
609 medium molecular size fraction of 3 to 30 kDa in spring, whereas in summer and autumn, low
610 (< 1-3 kDa) and heavy molecular weight fraction (30 kDa - 0.45µm) become highly abundant.
611 We revealed distinctly different behaviors of organo-ferric colloids in permafrost and non-
612 permafrost regions that are dependent upon the season. In continuous permafrost zones in spring,
613 there was a 2 to 3-fold increase in $LMW_{< 3\ kDa}$ OC relative to other permafrost zones. The
614 appearance of LMW OC north of 66°N during this period could be linked to full freezing of
615 small streams and generation of LMW organic ligands under freeze-thaw cycles. Fe
616 demonstrated distinctly different colloidal pattern depending on latitude and seasons: In
617 permafrost-free zone there was sizeable decrease of colloidal Fe, Al and trivalent hydrolysates
618 fraction in the course of the active season following the order spring > summer > autumn. In the
619 permafrost zone, the colloidal fraction of Fe, Al and Y, REE, Zr, Hf, Th^{+} was high (90±10%) in
620 spring but also decreasing to 60±20% in summer. Similarly, divalent metals (Cu, Co, Cd, Pb,

621 Mn) had the highest colloidal fraction in spring and the lowest in summer and autumn, across all
622 permafrost zones. These patterns were observed in all rivers regardless of their size and it could
623 be linked to progressive decrease of allochthonous terrestrial large size colloids that are being
624 replaced by small size aquagenic DOM and metal-DOM complexes.

625 The effect of river size was mostly pronounced in the permafrost-free zone consisting of
626 a decrease in colloidal DOC, Al, Fe, P, Ca, Mg and U in streams larger than 100 km² in watershed
627 area. In the permafrost zone, it was subordinate as compared to season and forest presence.
628 Although the size of the watershed exerted generally low impact on colloidal distribution, there
629 was a decrease in colloidal fraction of Al, P, Mg, Ca in rivers larger than 50,000 km² especially
630 in summer and autumn, probably linked to appearance of autochthonous LMW organic
631 complexes. The groundwater discharge of Fe(II), Ca, Mg, P, Mo, U ionic forms leading to
632 decrease in Fe colloids was visible in streams > 100 km² in the permafrost-free zone.

633 In continuous and discontinuous permafrost zones, the riverine colloids are delivered to
634 the river via lateral flow over suprapermafrost horizons, whereas in permafrost-free and sporadic
635 to isolated permafrost zones, delivery occurs via lateral surface runoff and riparian/hyporheic
636 discharge. Forest coverage increases connectivity with deep underground waters which in turn
637 enriches the river water with ionic forms of soluble elements in LMW (ionic) forms thereby
638 decreasing the fraction of colloids. Because the underground feeding of rivers by LMW forms
639 of soluble elements decreases from south to north in WSL, the relative proportion of colloids
640 increases northward. This underground discharge leads to a sizeable decrease of colloidal forms
641 of DOC, Al, Fe, P, alkaline-earths, Cu, Ni, As and U in summer and autumn as compared to
642 spring. This effect was strongly pronounced in the permafrost-free zone.

643 On a climate warming and further permafrost thaw perspective, the increase in depth of
644 the active layer and connectivity of a river with underground water reservoirs may decrease the
645 colloidal fraction of OC, Fe, Al and number of divalent and trivalent metals as well as tetravalent

hydrolysates in the sporadic and isolated permafrost zone which will become permafrost-free. The disappearance of continuous permafrost in the north will not sizeably impact colloidal status of elements in river water. The $LMW_{<3\ kDa}$ OC will likely decrease in spring but increase in summer and autumn. The forestation of wetlands and lake drainage may slightly diminish colloidal transport of DOC and metals at the expense of low molecular weight forms. Overall, given the significant role of seasonal and forestation effects on colloidal forms of OC and TE in WSL rivers, major changes in the colloidal nature of riverine C and nutrients under a climate warming scenario in the WSL are likely to be linked to change in vegetation (species, biomass and geographical extension) rather than temperature and hydrology.

Acknowledgements:
This work was supported by RSCF No 18-17-00237 "Mechanisms of hydrochemical runoff of the Ob river flood zone" (analyses, modeling), RFBR projects № 19-55-15002, RFBR № 18-35-00563\18, 17-05-00348_a, and a project of Ministry of Education and Science of the Russian Federation № 6.7515.2017/9.10.

References

Aiken G.R., Hsu-Kim H., Ryan J.N. (2011) Influence of dissolved oranic matter on the environmental fate of metals, nanoparticles, and colloids. *Environ. Sci. Technol.* **45**(8), 3196-3201.

Ala-Aho P., Soulsby C., Pokrovsky O.S., Kirpotin S.N., Karlsson J., Serikova S., Vorobyev S.N., Manasypov R.M., Loiko S., and Tetzlaff D. (2018a) Using stable isotopes to assess surface water source dynamics and hydrological connectivity in a high-latitude wetland and permafrost influenced landscape. *J. Hydrol*. 556, 279–293.

Ala-aho P., Soulsby C., Pokrovsky O.S., Kirpotin S.N., Karlsson J., Serikova S., Manasypov R., Lim A., Krickov I., Kolesnichenko L.G. (2018b) Permafrost and lakes control river isotope composition across a boreal Arctic transect in the Western Siberian lowlands. *Environ. Res. Lett.,* 13(3), doi: 10.1088/1748-9326/aaa4fe.

Aufdenkampe A.K., Mayorga E., Raymond P.A., Melack J.M., Doney S.C. et al. (2011) Riverine coupling of biogeochemical cycles between land, oceans, and atmosphere. *Front. Ecol. Environ*. **9**(1), 53-60.

Bagard M.L., Chabaux F., Pokrovsky O.S., Prokushkin A.S., Viers, J, Dupré B, Stille P. (2011) Seasonal variability of element fluxes in two Central Siberian rivers draining high latitude permafrost dominated areas. *Geochim. Cosmochim. Acta* **75,** 3335–3357.

Benoit G., Rozan T.F. (1999) The influence of size distribution on the particle concentration effect and trace metal partitioning in rivers. *Geochim. Cosmochim. Acta* **63**(1), 113-127.

Cuss C.W., Grant-Weaver I., Shotyk W. (2017) AF4-ICPMS with the 300 Da membrane to resolve metal-bearing 'colloids' < 1 kDa: optimization, fractogram decnvolution, and advanced quality control. *Anal. Chem.* **89**(15), 8027-8035.

Cuss C.W., Donner M.W., Grant-Weaver I., Noernberg T., Pelletier R., Sinnatamby R.N., Shotyk W. (2018) Measuring the distribution of trace elements amongst dissolved colloidal species as a fingerprint for contribution of tributaries to large boreal rivers. *Sci. Total Environ.* **642,** 1242-1251.

Dittmar Th., Kattner G. (2003) The biogeochemistry of the river and shelf ecosystem of the Arctic Ocean: a review. *Marine Chem.* **83,** 103-120.

Drake, T. W., Wickland, K. P., Spencer, R. G. M., McKnight, D. M. & Striegl, R. G. (2015) Ancient low-molecular-weight organic acids in permafrost fuel rapid carbon dioxide production upon thaw. *P. Natl. Acad. Sci. USA* **112,** 13946–13951.

Frey K.E., Siegel D.I., Smith L.C. (2007a) Geochemistry of west Siberian streams and their potential response to permafrost degradation. *Water Resources Res.* **43,** W03406, doi: 10.1029/2006WR004902.

Frey K.E., McClelland J.W., Holmes R.M., Smith L.C. (2007b) Impacts of climate warming and permafrost thaw on the riverine transport of nitrogen and phosphorus to the Kara Sea. *J. Geophys. Res.* **112,** G04S58, doi: 10.1029/2006JG000369.

Gordeev V.V., Martin J.M., Sidorov I.S., Sidorova M.V. (1996) A reassessment of the Eurasian river input of water, sediment, major elements, and nutrients to the Arctic ocean. *Amer. J. Sci.* **296,** 664-691.

Gordeev V.V., Rachold V., Vlasova I.E. (2004) Geochemical behavior of major an dtrace elements in suspended particulate material of the Irtysh river, the main tributary o fthe Ob river, Siberia. *Appl. Geochem.* **19,** 593-610.

Gottselig N., Amelung W., Kirchner J.W., Bol R., Eugster W. et al. (2017) Elemental composition of natural nanoparticles and fine colloids in European forest stream waters and their role as phosphorus carriers. *Global Biogeochem. Cycles* **31,** 1592-1607.

Holmes R.M., Peterson B.J., Gordeev V.V., Zhulidov A.V., Meybeck M., Lammers R.B., Vörösmarty C.J. (2000) Flux of nutrients from Russian rivers to the Arctic Ocean: Can we establish a baseline against which to judge future changes? *Water Resources Res.* **36**(8), 2309-2320.

Holmes R.M., Peterson B.J., Zhulidov A.V., Gordeev V.V., Makkaveev P.N., Stunzhas P.A., Kosmenko L.S., Köhler G.H., Shiklomanov A.I. (2001) Nutrient chemistry of the Ob' and Yenisey Rivers, Siberia: results from June 2000 expedition and evaluation of long-term data sets. *Marine Chem.* **75,** 219-227.

Holmes R.M., McClelland J.W., Peterson B.J., Tank S.E. et al. (2012) Seasonal and annual fluxes of nutrients and organic matter from large rivers to the Arctic Ocean and surrounding seas. *Estuaries Coasts* **35,** 369-382, doi: 10.1007/s12237-011-9386-6.

Ingri J., Widerlund A., Land M., Gustafsson O., Andersson P. and Ohlander B. (2000) Temporal variations in the fractionation of the rare earth elements in a boreal river; the role of colloidal particles. *Chem. Geol.,* **166,** 23–45.

Javed M.B., Cuss C.W., Grant-Weaver I., Shotyk W. (2017) Size-resolved Pb distribution in the Athabasca River shows snowmelt in the bituminous sands region an insignificant source of dissolved Pb. *Sci. Rep.* **7**, 43622, https://doi.org/1038/srep43622.

Koretsky C.M., Haas J. R., Ndenga, N.T., Miller, D. (2006) Seasonal variations in vertical redox stratification and potential influence on trace metal speciation in minerotrophic peat sediments. *Water Air Soil Pollut.* **173**(1-4), 373-403.

Krickov I., Lim A., Manasypov R.M., Loiko S.V., Shirokova L.S., Kirpotin S.N., Karlsson J., Pokrovsky O.S. (2018) Riverine particulate C and N generated at the permafrost

thaw front: case study of western Siberian rivers across a 1700-km latitudinal transect. *Biogeosciences* **15,** 6867–6884.

Krickov I., Lim A.G., Loiko S.V., Manasypov R.M., Vorobyev S.N., Shevchenko V.P., Gordeev V.V., Pokrovsky O.S. (2019) Major and trace elements in suspended matter of western Siberian rivers: first assessment across permafrost zones and landscape parameters of watersheds. *Geochim. Cosmochim. Acta,* submitted after revison.

Loiko S.V., Pokrovsky O.S., Raudina T.V., Lim A., Kolesnichenko L.G., Shirokova L.S., Vorobyev S.N., Kirpotin S.N. (2017). Abrupt permafrost collapse enhances organic carbon, CO_2, nutrient and metal release into surface waters. *Chem. Geol*. **471,** 153–165.

Lyvén B., Hassellöv M., Turner D.R., Haraldsson C., Andersson K. (2003) Competition between iron- and carbon-based colloidal carriers for trace metals in a freshwater assessed using flow field-flow fractionation coupled to ICPMS. *Geochim. Cosmochim. Acta,* **67,** 3791–3802.

Magritsky D.V. (2010) Annual suspended matter flow of the Russian rivers belonging to the Arctic Ocean basin and its anthropogenic transformation. *Vestnik Moscow State Univ. Ser. Geography* **5**(6), 17-24.

Mann, P.J., Eglinton T.I., McIntyre C.P., Zimov N., Davydova A., Vonk J.E., Holmes R.M., Spencer R.G.M. (2015) Utilization of ancient permafrost carbon in headwaters of Arctic fluvial networks. *Nat Commun* **6,** Art No 7856, doi: 10.1038/ncomms8856.

Nikitin S. P. and Zemtsov V. A. (1986) The variability of hydrological parameters of western Siberia, Nauka, Novosibirsk. pp. 204.

Oleinikova O.V., Drozdova O.Y., Lapitskiy S.A., Demin V.V., Bychkov A.Y., Ppkrovsky O.S. (2017a) Dissolved organic matter degradation by sunlight coagulates organo-mineral colloids and produces low-molecular weight fraction of metals in boreal humic waters. *Geochim. Cosmochim. Acta* **211,** 97–114.

Oleinikova O., Shirokova L.S., Gerard E., Drozdova O.Yu., Lapitsky S.A., Bychkov A.Y., Pokrovsky O.S. (2017b) Transformation of organo-ferric peat colloids by a heterotrophic bacterium. *Geochim. Cosmochim. Acta* **205,** 313–330.

Pawlowsky-Glahn V., (Editor), Buccianti, A. eds. (2011) Compositional Data Analysis: Theory and Applications. Wiley, 400 pp.

Philippe, A., & Schaumann, G. E. (2014). Interactions of dissolved organic matter with natural and engineered inorganic colloids: a review. *Environ. Sci. Technol.* **48**(16), 8946-8962.

Pokrovsky O.S., Schott J. (2002) Iron colloids/organic matter associated transport of major and trace elements in small boreal rivers and their estuaries (NW Russia). *Chem. Geol.* **190,** 141-179.

Pokrovsky O.S., Viers J., Shirokova L.S., Shevchenko V.P., Filipov A.S., Dupré B. (2010) Dissolved, suspended, and colloidal fluxes of organic carbon, major and trace elements in Severnaya Dvina River and its tributary. *Chem. Geol.* **273,** 136–149.

Pokrovsky O.S., Manasypov R.M., Shirokova L.S., Loiko S.V., Krickov I.V., Kopysov S. et al. (2015). Permafrost coverage, watershed area and season control of dissolved carbon and major elements in western Siberia rivers. *Biogeosciences* **12,** 6301–6320.

Pokrovsky O. S., Manasypov R.M., Loiko S.V., and Shirokova L.S. (2016a). Organic and organo-mineral colloids in discontinuous permafrost zone. *Geochim. Cosmochim. Acta* **188,** 1-20.

Pokrovsky O.S., Manasypov R.M., Loiko S., Krickov I.A., Kopysov S.G., Kolesnichenko L.G., Vorobyev S.N., Kirpotin S.N. (2016b) Trace element transport in western Siberia rivers across a permafrost gradient. *Biogeosciences* **13**(6), 1877–1900.

Pokrovsky, O.S., Karlsson J., and Giesler R. (2018) Freeze-thaw cycles of Arctic thaw ponds remove colloidal metals and generate low-molecular-weight organic matter. *Biogeochemistry* **137**(3), 321-336.

Pokrovsky O.S. (2019) Filtration and ultrafiltration results of western Siberian rivers. https://www.researchgate.net/publication/331928620_Colloidal_transport_of_carbon_and_metals_by_western_Siberian_rivers_Tab1, DOI: 10,13140 / RG.2.2.21502.64321.

Polishchuk Y.M., Bogdanov A.N., Polishchuk V.Y., Manasypov R.M., Shirokova L.S., Kirpotin S.N., Pokrovsky O.S. (2017) Size distribution, surface coverage, water, carbon, and metal storage of thermokarst lakes in the permafrost zone of the Western Siberia Lowland. *Water,* **9,** Art No 228; doi:10.3390/w9030228.

Porcelli D., Andersson P.S., Wasserburg G.J., Ingri J., Baskaran M., 1997. The importance of colloids and mires for the transport of uranium isotopes through the Kalix River watershed and Baltic Sea. *Geochim. Cosmochim. Acta* **61**(19), 4095–4113.

Raudina T.V, Loiko S.V., Lim A.G., Krickov I.V., Shirokova L.S., Istignichev G.I., Kuzmina D.M., Kulizhsky S.P., Vorobyev S.N., Pokrovsky O.S. (2017) Dissolved organic carbon and major and trace elements in peat porewater of sporadic, discontinuous, and continuous permafrost zones of western Siberia. *Biogeosciences* **14**(14), 3561–3584.

Raudina T.V., Loiko S.V., Lim A., Manasypov R.M., Shirokova L.S., Istigecgev G.I., Kuzmina D.M., Kulizhsky S.P., Vorobyev S.N., Pokrovsky O.S. (2018) Permafrost thaw and climate warming may decrease the CO_2, carbon, and metal concentration in peat soil waters of the Western Siberia Lowland. *Sci. Total Environ*. **634,** 1004-1023.

Riedel, Th., Zak, D., Dittmar, Th. (2013) Iron traps terrestrially derived dissolved organic matter at redox interfaces. *PNAS,* **110**(25), 10101-10105.

Rozan, T.F. and Benoit G. (1999) Geochemical factors controlling free Cu ion concentrations in river water. *Geochim. Cosmochim. Acta* **63**(19-20), 3311-3319.

Santana-Casiano J.M., Gonzalez-Davila M., Rodriguez M.J., Millero F.J. (2000) The effect of organic compounds in the oxidation kinetics of Fe(II). *Marine Chem*. **70** (1-3), 211-222.

Shim M.J., Cai Y., Guo L., Shiller A.M. (2017) Floodplain effects on the transport of dissolved and colloidal trace elements in the East Pearl River, Mississippi. *Hydrol. Proc.* **31**(5), 1086-1099.

Shirokova L.S., Pokrovsky O.S., Kirpotin S.N., Desmukh C., Pokrovsky B.G., Audry S., Viers J. (2013). Biogeochemistry of organic carbon, CO_2, CH_4, and trace elements in thermokarst water bodies in discontinuous permafrost zones of Western Siberia. *Biogeochemistry* **113,** 573-593.

Stolpe B., Guo L. and Shiller A. (2013a) Binding and transport of rare earth elements by organic and iron-rich nanocolloids in Alaskan rivers, as revealed by field-flow fractionation and ICP-MS. *Geochim. Cosmochim. Acta* **106,** 446-462.

Stolpe, B., Guo, L., Shiller, A. M., and Aiken, G. R. (2013b) Abundance, size distributions and trace-element binding of organic and iron-rich nanocolloids in Alaskan rivers, as revealed by field-flow fractionation and ICP-MS. *Geochim. Cosmochim. Acta* **105,** 221-239.

Tank S.E., Raymond P.A., Striegl R.G., McClelland J.W., Holmes R.M., Fiske G.J., and Peterson B.J. (2012) A land-to-ocean perspective on the magnitude, source and implication of DIC flux from major Arctic rivers to the Arctic Ocean. *Global Biogeochemical Cycles* **26,** GB4018.

Vasyukova E.V., Pokrovsky O.S., Viers J., Oliva P., Dupre B., Martin F., Candaudap F. (2010) Trace elements in organic- and iron-rich surficial fluids of the boreal zone: Assessing colloidal forms via dialysis and ultrafiltration. *Geochim. Cosmochim. Acta* **74**(2), 449-468.

Vorobyev S.N., Pokrovsky O.S., Serikova S., Manasypov R.M., Krickov I.V., Shirokova L.S., Lim A., Kolesnichenko L.G., Kirpotin S.N., Karlsson J. (2017) Permafrost boundary shift in western Siberia may not modify dissolved nutrient concentrations in rivers. *Water* **9**(12), 985, doi:10.3390/w9120985.

Walvoord M.A., Voss C.I., and Wellman, T. P. (2012) Influence of permafrost distribution on groundwater flow in the context of climate-driven permafrost thaw: Example from Yukon Flats Basin, Alaska, United States. *Water Res. Research,* **48,** W07524, doi:10.1029/2011WR011595.

Zhou, Z.Z., Stolpe, B., Guo, L.D., Shiller, A.M. (2016) Colloidal size spectra, composition and estuarine mixing behavior of DOM in river and estuarine waters of the northern Gulf of Mexico. *Geochim. Cosmochim. Acta* **181,** 1-17.

863 **Table 1.** Mean values of element concentrations in permafrost- bearing and permafrost-free zones of
864 western Siberian rivers. DOC is in mg L^{-1} and all other elements are in µg L^{-1}.

Mean	permafrost-free rivers (N = 2 to 7)					permafrost-bearing rivers (N = 6 to 25)				
Size fraction	**1 kDa**	**3 kDa**	**30 kDa**	**100 kDa**	**0.45 µm**	**1 kDa**	**3 kDa**	**30 kDa**	**10 kDa**	**0.45 µm**
DOC (Spring)	N.D.	4.57	22.3	22.0	18.8	N.D.	3.61	8.69	9.26	9.51
DOC (Summer)	N.D.	7.98	13.4	13.9	14.1	2.74	4.29	7.09	7.38	7.67
DOC (Autumn)	6.751	5.63	8.29	10.0	10.6	2.91	3.45	8.49	N.D.	8.80
Li (Spring)	N.D.	1.45	1.73	8.08	2.71	N.D.	0.794	0.870	1.14	0.836
Li (Summer)	N.D.	3.32	3.32	3.07	3.04	1.76	2.16	2.34	2.33	2.27
Li (Autumn)	2.73	3.34	3.46	1.99	3.18	1.52	1.71	1.82	N.D.	1.82
B (Spring)	N.D.	13.1	11.9	12.0	15.0	N.D.	7.86	8.18	8.17	7.87
B (Summer)	N.D.	42.9	42.3	33.9	35.3	10.2	27.4	30.7	30.2	28.9
B (Autumn)	31.85	45.0	47.9	7.00	36.9	10.4	13.0	12.2	N.D.	13.0
Na (Spring)	N.D.	2042	2377	2457	3068	N.D.	1754	1717	1744	1769
Na (Summer)	N.D.	8932	10026	7739	7496	2689	4207	4755	4745	4850
Na (Autumn)	6911	9870	11556	1491	8644	2920	4169	3846	N.D.	4459
Mg (Spring)	N.D.	2447	2607	2628	3284	N.D.	619	807	811	827
Mg (Summer)	N.D.	13110	12623	10169	10686	2258	2271	2599	2577	2569
Mg (Autumn)	11537	14691	14997	2382	12055	2664	1907	2168	N.D.	2091
Al (Spring)	N.D.	17.1	94.0	105	79.3	N.D.	11.1	62.8	64.9	64.3
Al (Summer)	N.D.	18.1	16.7	22.9	26.3	2.55	4.64	17.3	18.3	21.3
Al (Autumn)	5.75	4.95	8.14	10.5	7.28	5.50	12.5	37.8	N.D.	39.6
Si (Spring)	N.D.	2189	1999	2041	2434	N.D.	1977	1998	1968	2009
Si (Summer)	N.D.	7810	7010	6324	6334	6486	5408	5559	5495	5596
Si (Autumn)	5655	7775	6819	4615	6563	6474	5660	5742	N.D.	5662
P (Spring)	N.D.	30.8	39.6	44.6	53.6	N.D.	10.7	18.3	20.5	18.6
P (Summer)	N.D.	40.7	48.9	59.3	62.6	13.6	16.9	27.5	28.3	32.9
P (Autumn)	1.71	30.5	35.1	23.7	32.3	9.539	13.6	20.3	N.D.	19.4
K (Spring)	N.D.	1265	1286	1325	1496	N.D.	191	252	252	242
K (Summer)	N.D.	1317	1351	1636	1448	475	569	677	673	633
K (Autumn)	1326	1316	1378	3252	1656	492	375	435	N.D.	408
Ca (Spring)	N.D.	13002	13696	13871	18681	N.D.	1104	1552	1565	1770
Ca (Summer)	N.D.	63988	59880	49260	53383	5666	5166	5631	5585	5903
Ca (Autumn)	55525	69166	67320	12700	57826	6120	4169	4583	N.D.	4787
Ti (Spring)	N.D.	2.53	5.07	5.88	6.54	N.D.	2.25	3.30	3.67	3.82
Ti (Summer)	N.D.	6.19	6.22	5.49	5.38	5.10	4.70	5.05	5.02	5.77
Ti (Autumn)	0.504	0.685	0.634	0.440	0.595	0.581	0.532	0.652	N.D.	0.686
V (Spring)	N.D.	0.428	0.654	0.710	0.650	N.D.	0.277	0.374	0.390	0.363
V (Summer)	N.D.	0.630	0.893	0.787	0.787	0.319	0.236	0.285	0.294	0.351
V (Autumn)	0.423	0.362	0.490	0.362	0.513	0.338	0.300	0.354	N.D.	0.352
Cr (Spring)	N.D.	0.0349	0.322	0.322	0.277	N.D.	0.464	0.681	0.701	0.673
Cr (Summer)	N.D.	0.159	0.217	0.173	0.219	0.0705	0.0828	0.146	0.178	0.206
Cr (Autumn)	0.169	0.133	0.183	0.111	0.181	0.257	0.286	0.540	N.D.	0.496
Mn (Spring)	N.D.	5.04	6.81	9.95	10.3	N.D.	15.8	24.7	25.9	42.3
Mn (Summer)	N.D.	47.7	23.5	5.93	62.8	0.578	53.3	56.4	55.0	66.3
Mn (Autumn)	0.485	11.8	0.581	0.474	9.96	11.07	51.5	56.7	N.D.	74.7
Fe (Spring)	N.D.	9.16	189	237	236	N.D.	7.30	145	199	254
Fe (Summer)	N.D.	32.2	59.1	59.1	198	4.90	7.81	52.2	69.4	192
Fe (Autumn)	22.1	29.2	33.2	9.94	61.4	3.68	8.70	75.4	N.D.	199
Co (Spring)	N.D.	0.0274	0.0936	0.107	0.0951	N.D.	0.0493	0.121	0.125	0.196
Co (Summer)	N.D.	0.0767	0.126	0.0897	0.171	0.0210	0.0843	0.136	0.133	0.170
Co (Autumn)	0.100	0.0635	0.119	0.0277	0.102	0.0292	0.0947	0.189	N.D.	0.213
Ni (Spring)	N.D.	0.485	1.91	1.94	1.62	N.D.	0.529	0.972	1.06	0.943
Ni (Summer)	N.D.	1.87	1.75	1.58	1.28	0.173	0.310	0.666	0.776	0.705
Ni (Autumn)	0.753	0.564	0.932	0.445	0.865	0.236	0.310	0.852	N.D.	0.753
Cu (Spring)	N.D.	0.263	1.31	1.36	1.45	N.D.	0.1419	0.540	0.518	0.530
Cu (Summer)	N.D.	0.501	1.13	1.05	0.785	0.101	0.153	0.361	0.381	0.341
Cu (Autumn)	0.494	0.288	0.463	0.267	0.524	0.185	0.139	0.388	N.D.	0.321

Mean	permafrost-free rivers (N = 2 to 7)					permafrost-bearing rivers (N = 6 to 25)				
Size fraction	**1 kDa**	**3 kDa**	**30 kDa**	**100 kDa**	**0.45 µm**	**1 kDa**	**3 kDa**	**30 kDa**	**10 kDa**	**0.45 µm**
Zn (Spring)	N.D.	0.805	2.11	2.06	4.61	N.D.	1.88	3.04	2.98	3.50
Zn (Summer)	N.D.	0.573	0.705	0.596	1.26	1.21	1.39	1.14	0.968	1.58
Zn (Autumn)	0.235	0.185	N.D.	1.11	0.560	0.639	0.706	1.05	N.D.	1.09
Ga (Spring)	N.D.	0.00275	0.00516	0.00699	0.00674	N.D.	0.00665	0.00925	0.0102	0.0105
Ga (Summer)	N.D.	0.0136	0.00721	0.00470	0.0121	0.000936	0.00733	0.00720	0.00758	0.00914
Ga (Autumn)	0.00613	0.00377	0.00559	0.00266	0.00479	0.00513	0.00748	0.00893	N.D.	0.00988
As (Spring)	N.D.	0.511	0.832	0.867	0.879	N.D.	0.243	0.356	0.363	0.382
As (Summer)	N.D.	0.996	1.32	1.26	1.29	0.386	0.341	0.451	0.449	0.500
As (Autumn)	0.590	0.522	0.705	0.325	0.765	0.252	0.219	0.313	N.D.	0.314
Rb (Spring)	N.D.	0.900	1.05	1.07	1.01	N.D.	0.292	0.409	0.406	0.390
Rb (Summer)	N.D.	1.22	1.22	1.38	1.21	0.689	0.689	0.801	0.799	0.747
Rb (Autumn)	1.09	1.10	1.13	2.48	1.28	0.665	0.447	0.525	N.D.	0.503
Sr (Spring)	N.D.	66.6	71.8	72.9	94.5	N.D.	8.08	10.7	10.7	12.7
Sr (Summer)	N.D.	346	336	271	283	30.7	129	146	142	134
Sr (Autumn)	319	394	405	51.2	326	28.9	34.5	28.2	N.D.	38.9
Y (Spring)	N.D.	0.0114	0.241	0.267	0.182	N.D.	0.0229	0.180	0.193	0.186
Y (Summer)	N.D.	0.0138	0.0335	0.0270	0.0355	0.00348	0.00988	0.0385	0.0428	0.0559
Y (Autumn)	0.00726	0.00695	0.0148	0.00494	0.0182	0.00335	0.0193	0.115	N.D.	0.122
Zr (Spring)	N.D.	0.00325	0.201	0.220	0.172	N.D.	0.00296	0.103	0.113	0.111
Zr (Summer)	N.D.	0.0113	0.0901	0.0649	0.0709	0.00152	0.00334	0.0483	0.0512	0.0745
Zr (Autumn)	0.00725	0.00262	0.0220	0.000743	0.0251	0.00136	0.00341	0.109	N.D.	0.121
Mo (Spring)	N.D.	0.202	0.284	0.294	0.278	N.D.	0.0108	0.0161	0.0159	0.0179
Mo (Summer)	N.D.	0.221	0.350	0.301	0.294	0.0319	0.0254	0.0317	0.0337	0.0309
Mo (Autumn)	0.304	0.166	0.262	0.263	0.278	0.0296	0.0160	0.0197	N.D.	0.0185
Cd (Spring)	N.D.	0.00251	0.00912	0.0102	0.0118	N.D.	0.00320	0.00662	0.00714	0.00728
Cd (Summer)	N.D.	0.00543	0.00297	0.00989	0.00833	0.00346	0.00430	0.00491	0.00531	0.00841
Cd (Autumn)	0.000754	0.000837	0.00146	0.000630	0.00182	0.00553	0.00243	0.00400	N.D.	0.00481
Sb (Spring)	N.D.	0.0616	0.0826	0.0670	0.0838	N.D.	0.0220	0.0272	0.0287	0.0272
Sb (Summer)	N.D.	0.0434	0.0670	0.0563	0.0539	0.0148	0.0182	0.0204	0.0222	0.0183
Sb (Autumn)	0.0514	0.0283	0.0478	0.0251	0.0431	0.0121	0.0165	0.0204	N.D.	0.0192
Ba (Spring)	N.D.	15.4	19.3	20.0	23.2	N.D.	3.17	5.26	5.47	6.23
Ba (Summer)	N.D.	50.5	43.4	35.3	42.2	5.52	25.7	38.3	28.0	27.3
Ba (Autumn)	23.9	45.5	37.7	7.53	38.0	4.93	8.10	7.48	N.D.	10.3
La (Spring)	N.D.	0.0355	0.226	0.244	0.185	N.D.	0.0412	0.141	0.173	0.179
La (Summer)	N.D.	N.D.	N.D.	N.D.	0.0242	0.0804	0.0499	0.0667	0.0438	0.0610
La (Autumn)	0.00626	0.00263	0.00430	0.00416	0.00759	0.00369	0.0207	0.125	N.D.	0.143
Ce (Spring)	N.D.	0.00955	0.299	0.360	0.260	N.D.	0.0350	0.286	0.312	0.315
Ce (Summer)	N.D.	0.0120	0.0390	0.0221	0.0303	0.0110	0.0126	0.0752	0.0547	0.0692
Ce (Autumn)	0.00181	0.00115	0.00226	0.00403	0.00787	0.00327	0.0275	0.141	N.D.	0.156
Pr (Spring)	N.D.	0.00153	0.0462	0.0534	0.0438	N.D.	0.00472	0.0373	0.0414	0.0396
Pr (Summer)	N.D.	0.000579	0.00289	0.00307	0.00505	0.000536	0.00160	0.00550	0.00593	0.00888
Pr (Autumn)	0.000123	0.000140	0.000514	0.00103	0.00174	0.000277	0.00341	0.0196	N.D.	0.0221
Nd (Spring)	N.D.	0.00722	0.196	0.221	0.188	N.D.	0.02019	0.161	0.175	0.166
Nd (Summer)	N.D.	0.00283	0.0140	0.0132	0.0229	0.00234	0.00700	0.0237	0.0247	0.0395
Nd (Autumn)	0.000497	0.00155	0.00189	0.00370	0.00768	0.00174	0.0162	0.0870	N.D.	0.0964
Sm (Spring)	N.D.	0.00160	0.0463	0.0519	0.0431	N.D.	0.00469	0.0358	0.0401	0.0394
Sm (Summer)	N.D.	0.00121	0.00507	0.00301	0.00517	0.00105	0.00183	0.00563	0.00645	0.00942
Sm (Autumn)	0.000448	0.000800	0.000759	0.000656	0.00212	0.000275	0.00355	0.0204	N.D.	0.0223
Gd (Spring)	N.D.	0.00168	0.0471	0.0558	0.0470	N.D.	0.00453	0.0387	0.0419	0.0408
Gd (Summer)	N.D.	0.00194	0.00520	0.00407	0.00632	0.000640	0.00187	0.00667	0.00700	0.00972
Gd (Autumn)	0.000729	0.000973	0.00226	0.000720	0.00262	0.000518	0.00359	0.0221	N.D.	0.0241
Dy (Spring)	N.D.	0.00175	0.0403	0.0443	0.0402	N.D.	0.00360	0.0323	0.0351	0.0340
Dy (Summer)	N.D.	0.00186	0.00461	0.00385	0.00525	0.000541	0.00160	0.00612	0.00685	0.00930
Dy (Autumn)	0.000632	0.000538	0.000619	0.000630	0.00197	0.000218	0.00287	0.0194	N.D.	0.0215
Yb (Spring)	N.D.	0.000922	0.0204	0.0226	0.0215	N.D.	0.00270	0.0183	0.0196	0.0186
Yb (Summer)	N.D.	0.00114	0.00352	0.00316	0.00359	0.00114	0.00119	0.00501	0.00525	0.00679
Yb (Autumn)	0.000828	0.000744	0.00129	0.00068	0.00167	0.000610	0.00229	0.0134	N.D.	0.0143

Mean	permafrost-free rivers (N = 2 to 7)					permafrost-bearing rivers (N = 6 to 25)				
Size fraction	**1 kDa**	**3 kDa**	**30 kDa**	**100 kDa**	**0.45 µm**	**1 kDa**	**3 kDa**	**30 kDa**	**10 kDa**	**0.45 µm**
Hf (Spring)	N.D.	0.00109	0.0278	0.0296	0.0226	N.D.	0.00110	0.0153	0.01617	0.0168
Hf (Summer)	N.D.	0.00342	0.00669	0.00496	0.00713	0.00104	0.00172	0.00849	0.00874	0.0103
Hf (Autumn)	0.000907	0.000794	0.00354	0.00141	0.00247	0.000705	0.000701	0.0109	N.D.	0.0117
Pb (Spring)	N.D.	0.00875	0.0598	0.0700	0.457	N.D.	0.0156	0.0409	0.0504	0.0626
Pb (Summer)	N.D.	0.0665	N.D.	0.00867	0.0156	0.01556	0.0362	0.0459	0.0629	0.0613
Pb (Autumn)	N.D.	0.00591	0.00379	N.D.	0.00318	0.0258	0.00922	0.0111	N.D.	0.0256
Th (Spring)	N.D.	0.000392	0.0325	0.0363	0.0273	N.D.	0.000674	0.0158	0.0161	0.0164
Th (Summer)	N.D.	0.000267	0.00332	0.00167	0.00319	0.000296	0.000283	0.00417	0.00473	0.00584
Th (Autumn)	0.000251	0.0000645	0.000349	0.0000300	0.000937	0.000431	0.000611	0.0117	N.D.	0.0129
U (Spring)	N.D.	0.0289	0.0759	0.0792	0.177	N.D.	0.000705	0.00954	0.00963	0.00908
U (Summer)	N.D.	0.189	0.287	0.227	0.254	0.00416	0.00202	0.00529	0.00533	0.00708
U (Autumn)	0.331	0.184	0.264	0.001592	0.249	0.00554	0.00203	0.00846	N.D.	0.00801

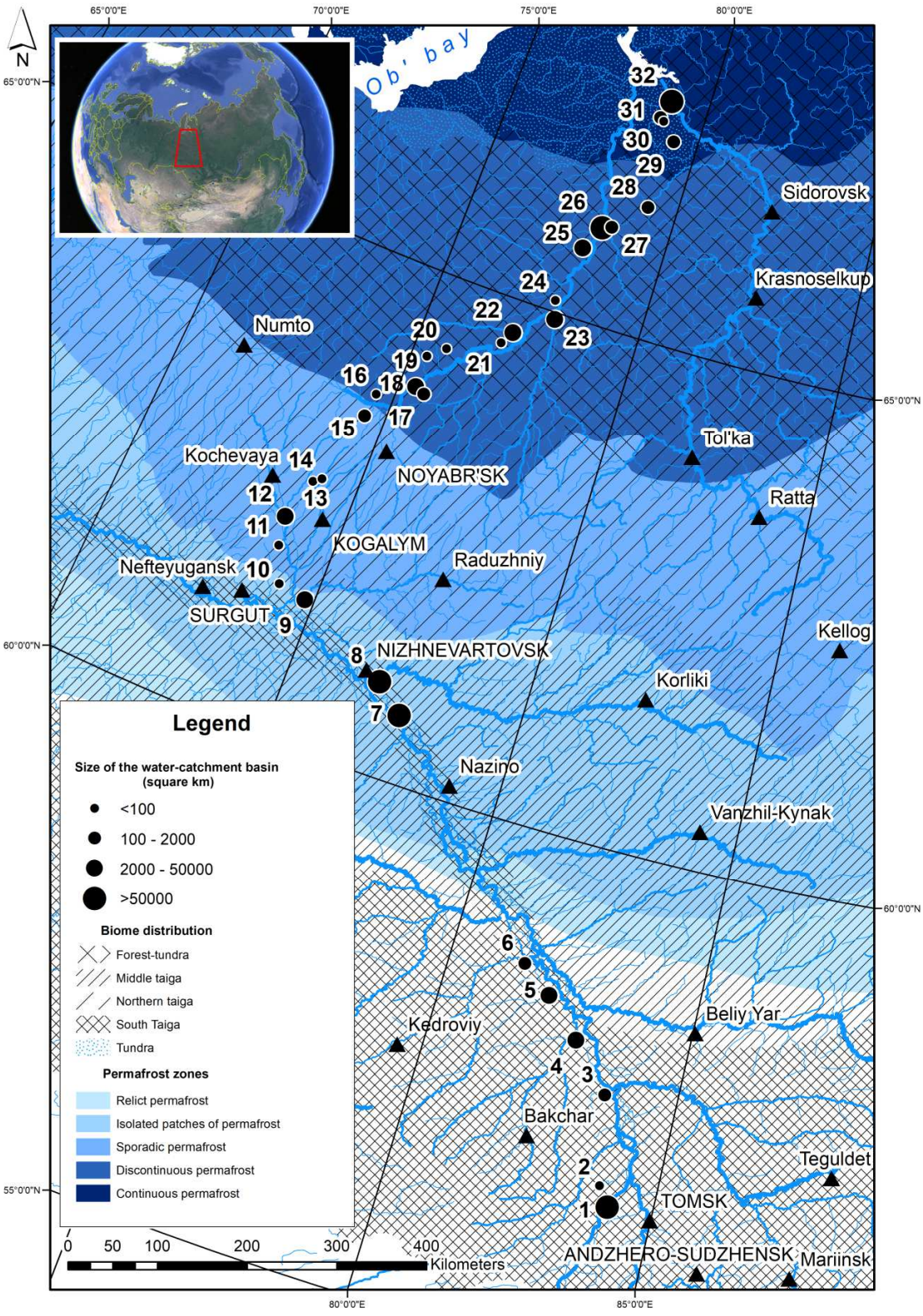

Fig. 1. A map of sampled rivers in Western Siberian Lowland. The latitudinal gradient covers 1700 km traversing taiga, forest-tundra and tundra of permafrost-free, sporadic, isolated, discontinuous and continuous permafrost zones. All the primary data on major and trace element concentration in 0.45 µm, 1 kDa, 3 kDa, 30 kDa and 100 kDa size fraction are available from https://www.researchgate.net/publication/331928620; doi: 10.13140/RG.2.2.21502.64321.

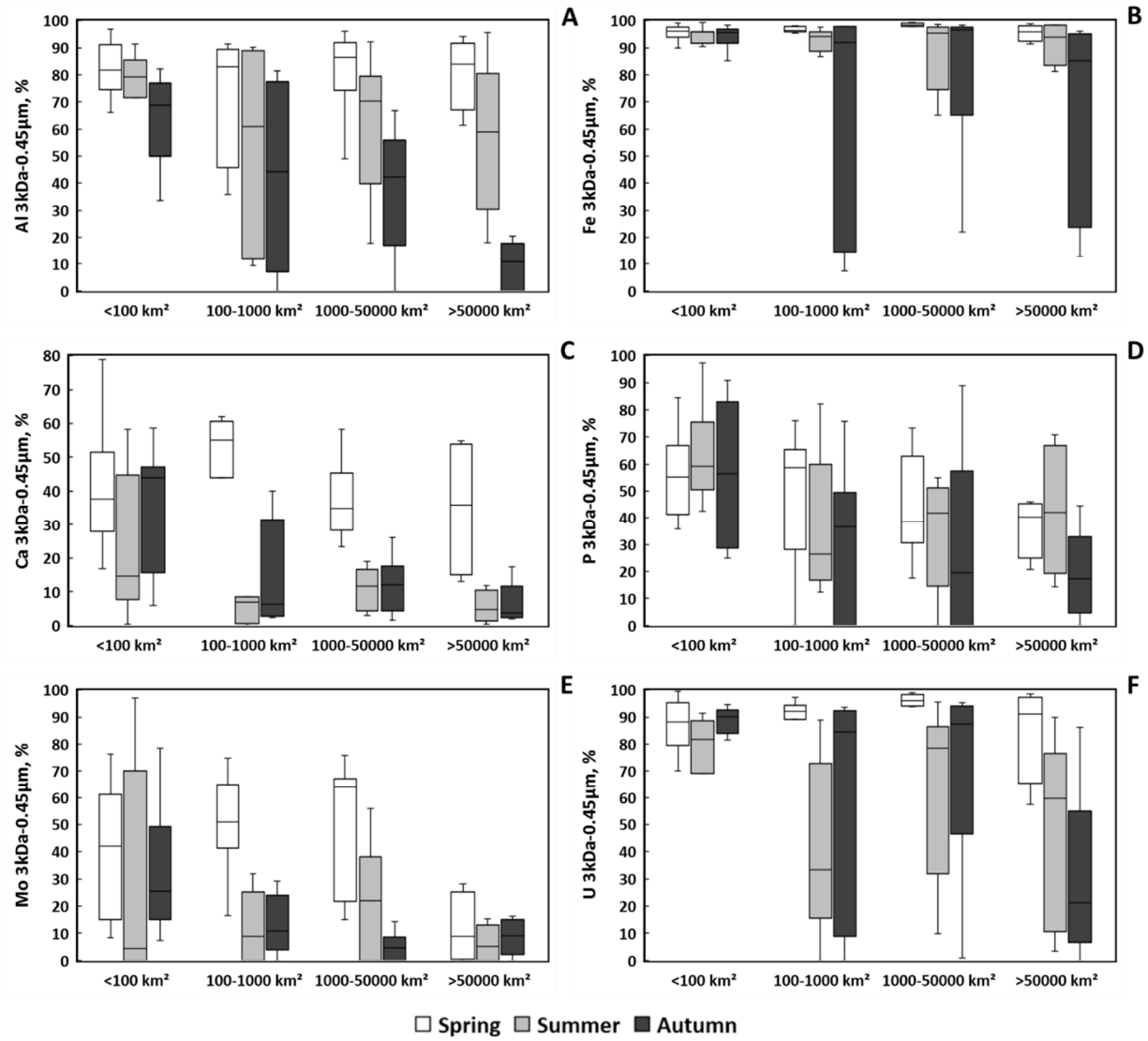

Fig. 2. Box plot of first and third quartiles (25 and 75%) of colloidal (3 kDa - 0.45 µm) proportion of Al (A), Fe (B), Ca (C), P (D), Mo (E) and U (F) in WSL rivers of different watershed size, during spring (blue), summer (red) and autumn (green). Here and in figures below, all 32 rivers from the 5 permafrost zones are included here.

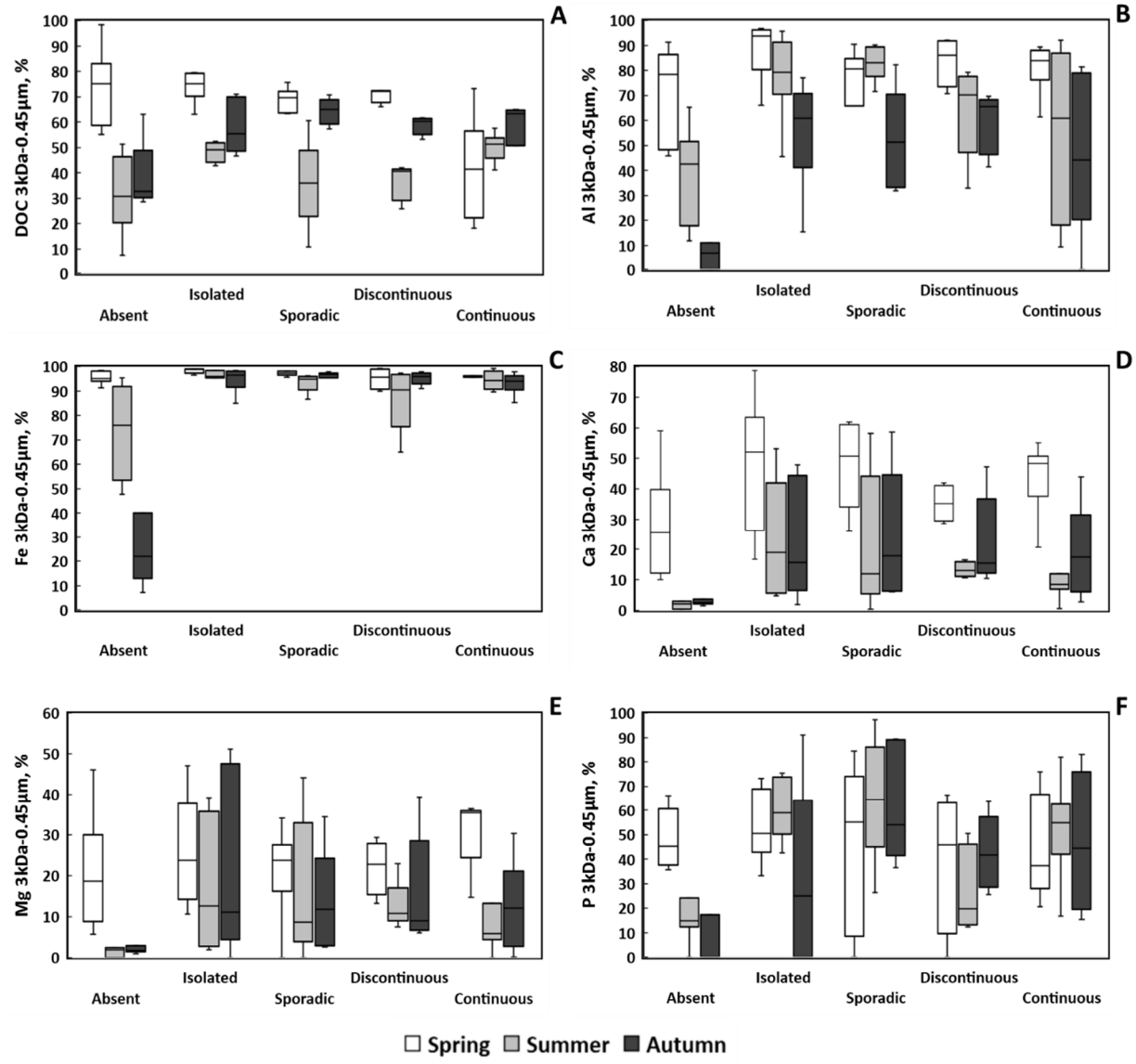

Fig. 3. Box plot of first and third quartiles (25 and 75%) of colloidal (3 kDa - 0.45 µm) proportion of OC (A), Al (B), Fe (C), Ca (D), Mg (E) and P (F) in WSL rivers of different permafrost zones, during spring (blue), summer (red) and autumn (green).

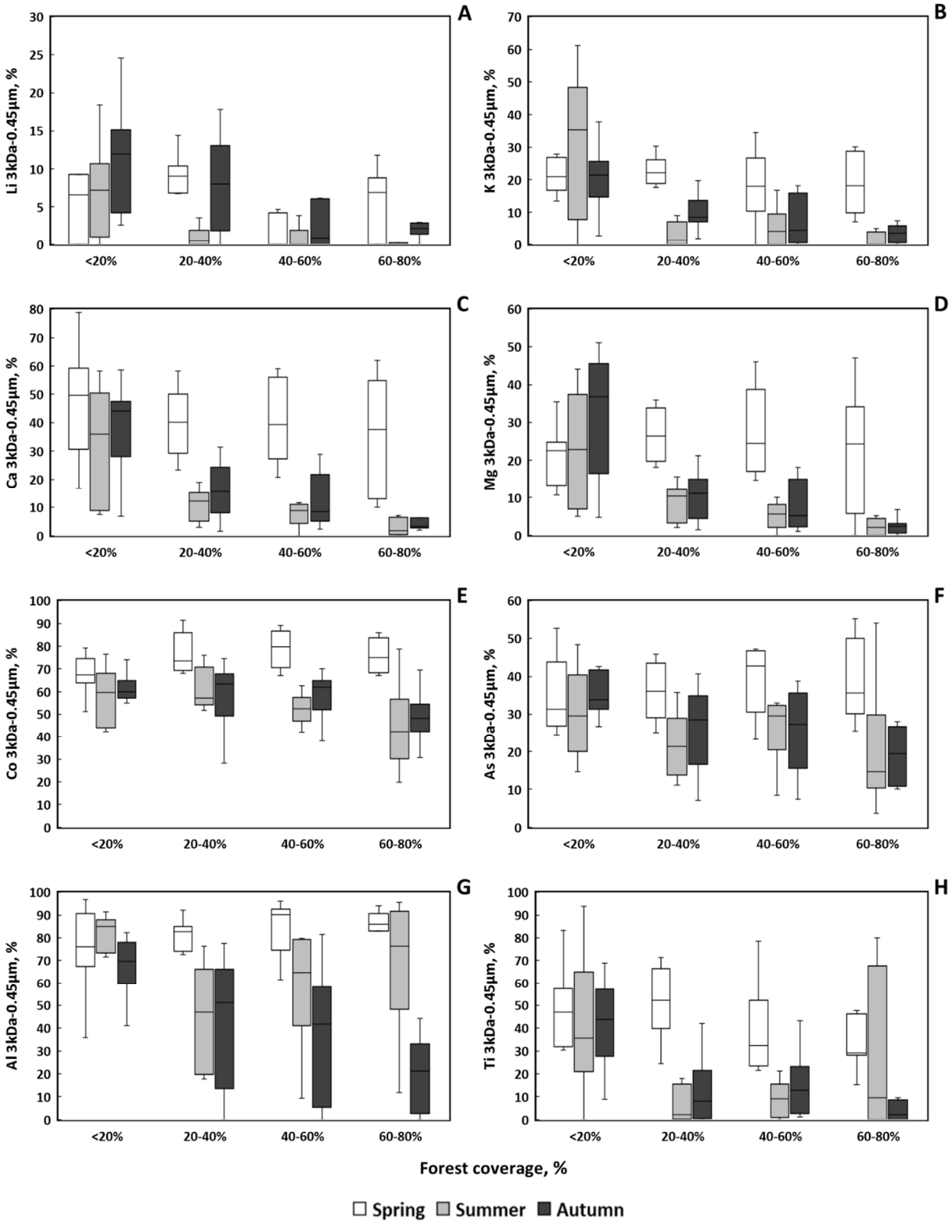

915

916

917 **Fig. 4.** Box plot of first and third quartiles (25 and 75%) of colloidal (3 kDa - 0.45 µm) proportion
918 of Li (A), K (B), Ca (C), Mg (D), Co (E), As (F), Al (G) and Ti (H) in WSL rivers with different
919 forest coverage, during spring (blue), summer (red) and autumn (green).

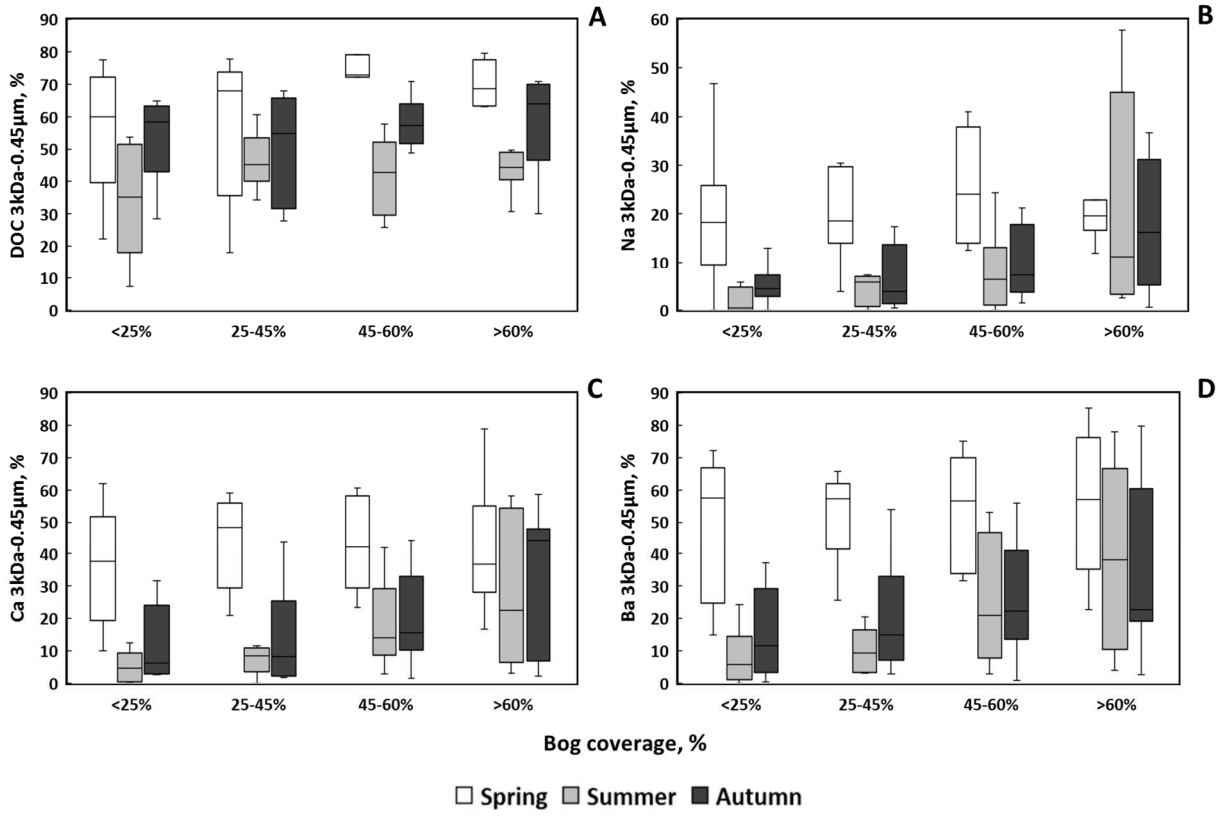

Fig. 5. Box plot of first and third quartiles (25 and 75%) of colloidal (3 kDa - 0.45 µm) proportion of DOC (A), Na (B), Ca (C), and Ba (D) in WSL rivers of different bog coverage, during spring (blue), summer (red) and autumn (green).

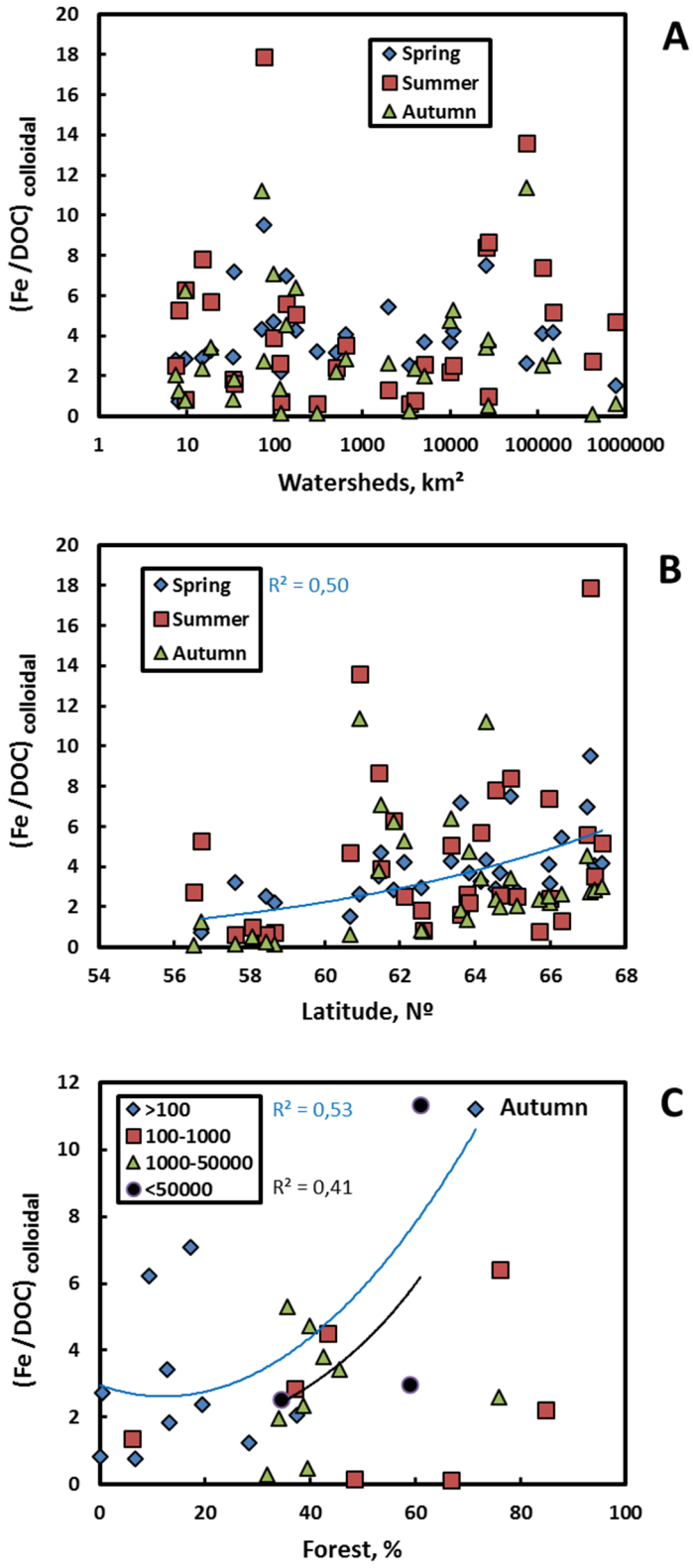

931

932

933 **Fig. 6.** Mass ratio of Fe to C in colloidal (3 kDa - 0.45 µm) fraction as a function of watershed
934 area (A), latitude (B) and forest coverage (C) of the watershed. Spring, summer and autumn
935 periods are shown by diamonds, squares and triangles, respectively.

936

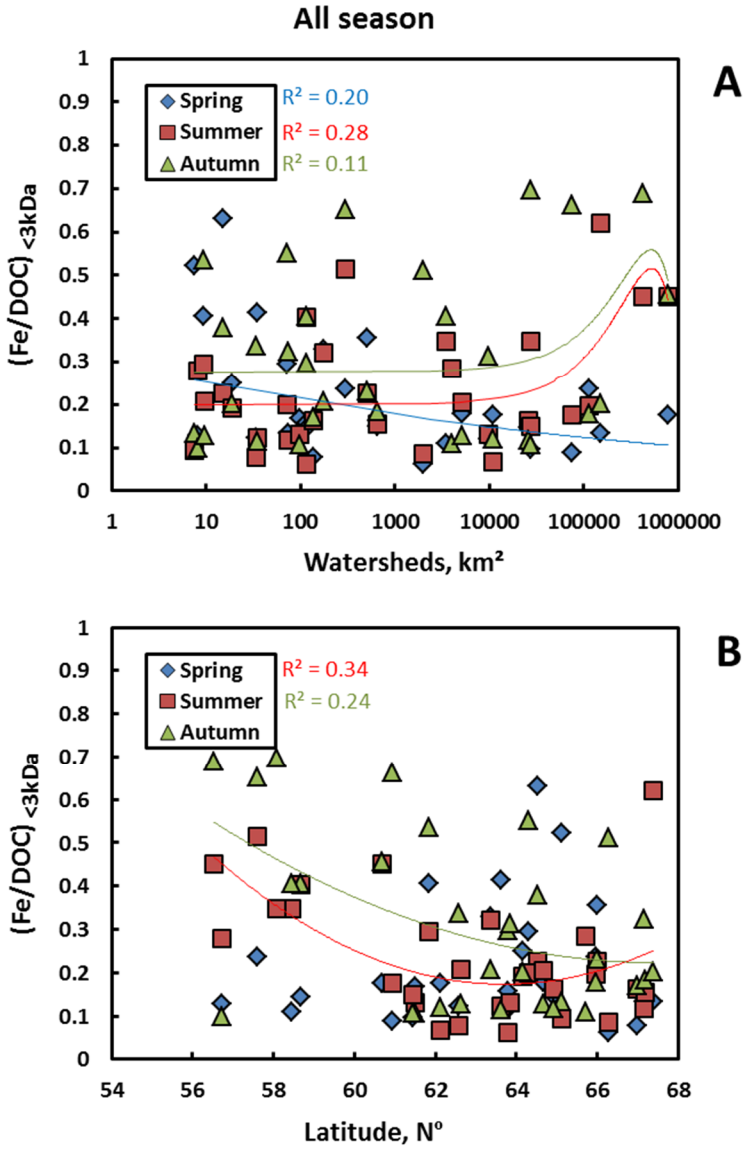

Fig. 7. Mass ratio of Fe to C in $LMW_{< 3\ kDa}$ fraction (ppm:ppm × 100) as a function of watershed area (A) and forest coverage of the watershed (B). Spring, summer and autumn periods are shown by diamonds, squares and triangles, respectively.

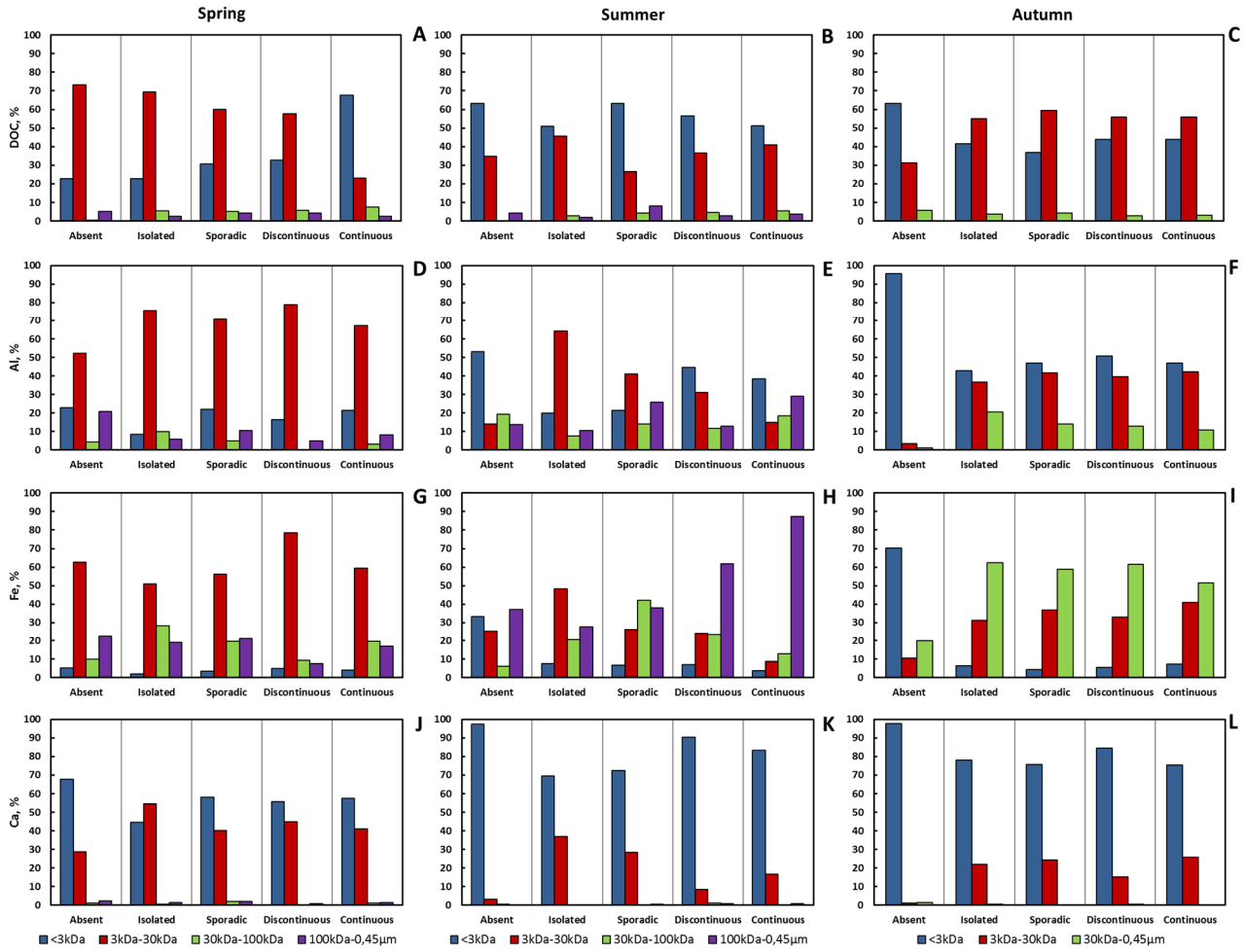

Fig. 8. Histogram of LMW and colloidal form distribution among 3 main colloidal and LMW$_{<3\ kDa}$ pools of DOC (A-C); Al (D-F); Fe (G-I); and Ca (J-L) in spring, summer and autumn for permafrost-free and 4 permafrost zones of WSL rivers.

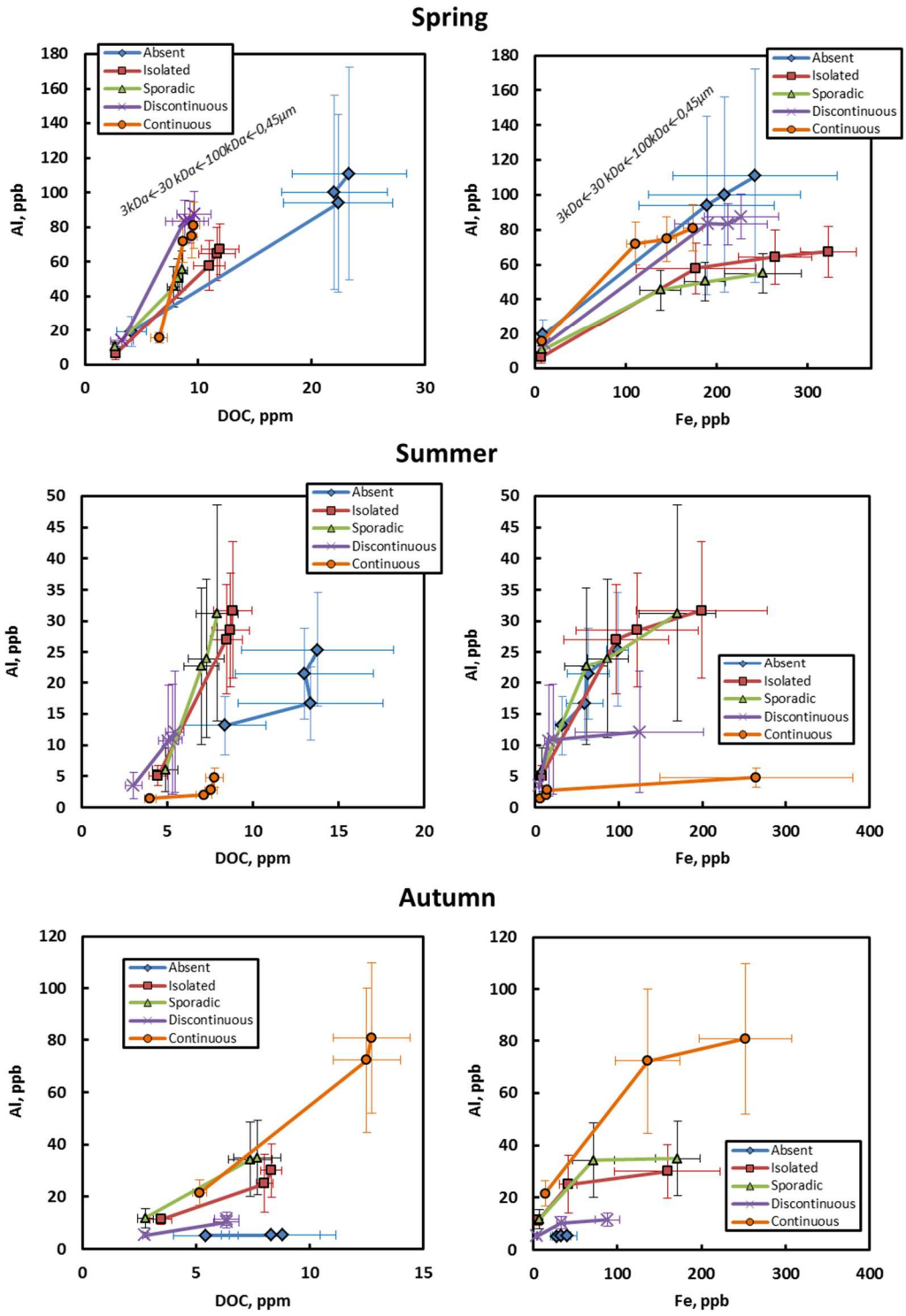

Fig. 9. Concentration pattern of Al, Fe and DC during colloidal separation by filtration through 0.45 µm and further ultrafilration through 100, 30 and 3 kDa. Shown are average values of rivers located in each permafrost zone in the three main seasons. The vertical and horizontal uncertainties of the average for several rivers (3 in permafrost-free zone, 5 in isolated, 9 in sporadic, 4 in discontinuous and 5 in continuous permafrost zone).

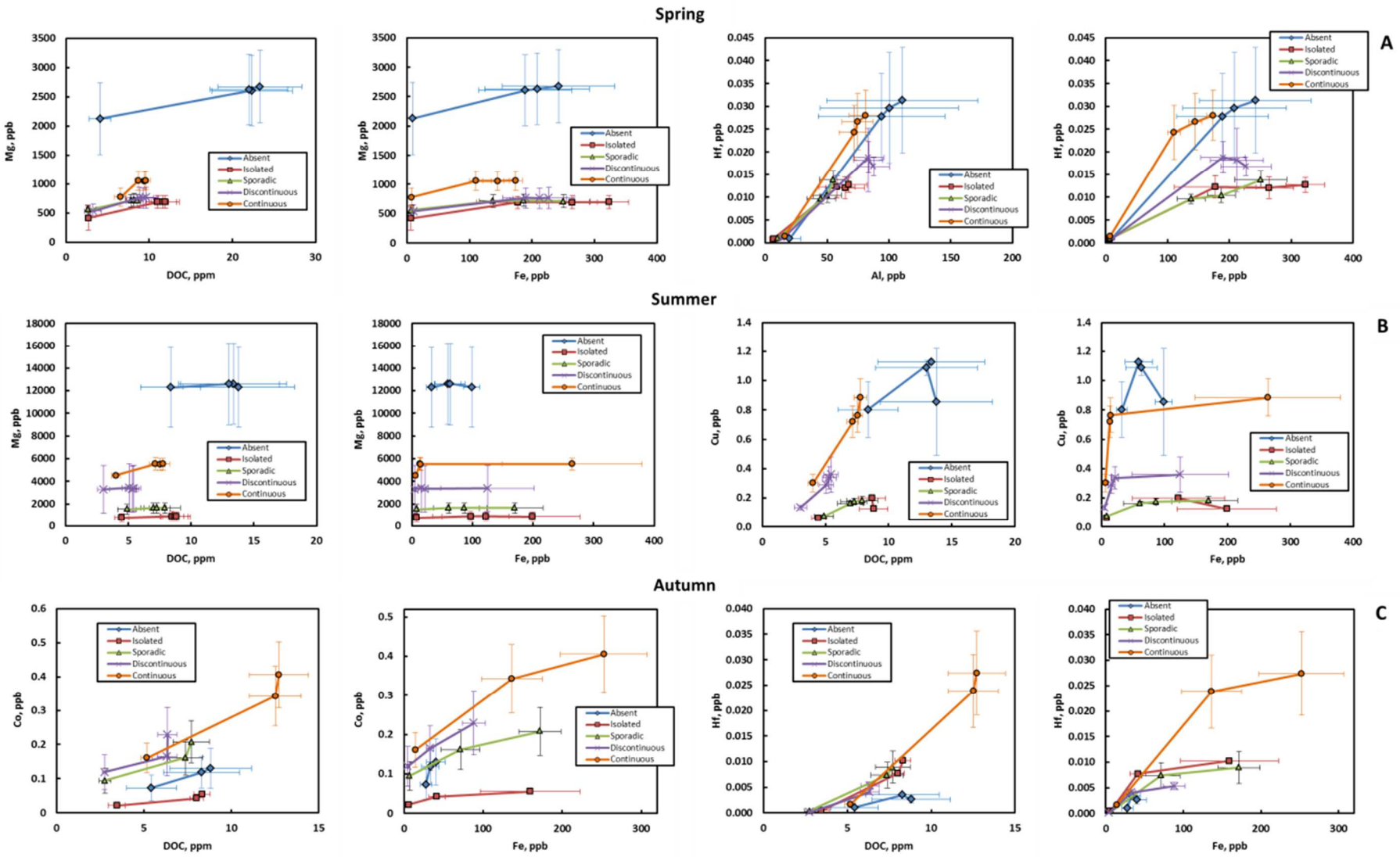

969

970 **Fig. 10.** Concentration pattern of selected elements (Mg, Cu, Co, Hf, Th) vs DOC or Fe during colloidal separation by filtration through 0.45 µm and
971 further ultrafiltration through 100, 30 and 3 kDa. Shown are average values of rivers located in each permafrost zone in spring (A), summer (B) and
972 autumn (C).